ANL-6619

ANL-6619

Argonne National Laboratory

REACTOR DEVELOPMENT PROGRAM

PROGRESS REPORT

September 1962

ANL-6619
Reactor Technology
(TID-4500, 18th Ed.)
AEC Research and
Development Report

ARGONNE NATIONAL LABORATORY
9700 South Cass Avenue
Argonne, Illinois

REACTOR DEVELOPMENT PROGRAM PROGRESS REPORT

September 1962

Albert V. Crewe, Laboratory Director

Division	Director
Chemical Engineering	S. Lawroski
Idaho	M. Novick
Metallurgy	F. G. Foote
Reactor Engineering	B. I. Spinrad
Remote Control	R. C. Goertz

Report coordinated by R. M. Adams

Issued October 15, 1962

Operated by The University of Chicago
under
Contract W-31-109-eng-38
with the
U. S. Atomic Energy Commission

FOREWORD

The Reactor Development Program Progress Report, issued monthly, is intended to be a means of reporting those items of significant technical progress which have occurred in both the specific reactor projects and the general engineering research and development programs. The report is organized in a way which, it is hoped, gives the clearest, most logical over-all view of progress. The budget classification is followed only in broad outline, and no attempt is made to report separately on each sub-activity number. Further, since the intent is to report only items of significant progress, not all activities are reported each month. In order to issue this report as soon as possible after the end of the month editorial work must necessarily be limited. Also, since this is an informal progress report, the results and data presented should be understood to be preliminary and subject to change unless otherwise stated.

The issuance of these reports is not intended to constitute publication in any sense of the word. Final results either will be submitted for publication in regular professional journals or will be published in the form of ANL topical reports.

The last six reports issued
in this series are:

March 1962	ANL-6544
April 1962	ANL-6565
May 1962	ANL-6573
June 1962	ANL-6580
July 1962	ANL-6597
August 1962	ANL-6610

TABLE OF CONTENTS

TABLE OF CONTENTS

TABLE OF CONTENTS

I. WATER COOLED REACTORS

A. EBWR

Additions and modifications to the EBWR plant have been completed which permit heat dissipation at power levels up to 100 Mwt. The plant has been authorized to operate at its full capacity and operational testing at the 60 Mwt level has been reached.

The composition of the current core fuel loading (Core 1A) consists of the following:

Subassembly Type	Number
Spike	32
Natural Uranium (thick plate)	8
Natural Uranium (thin plate)	1
1.44% Enriched (thick plate)	52
1.44% Enriched (thin plate)	54
Total Number of Subassemblies	147

The nominal diameter of the core is 5 ft and the inside diameter of the reactor vessel is 7 ft. There is approximately 8 ft of water above the core, 7 ft between the cold water level and the top of the reactor vessel. Thus, the downcomer flow rate, steam separation characteristics, and carryunder experienced in these tests are in part due to the geometrical arrangement of the particular system. Modifications to the system are thus limited in certain instances by the particular features of the components in the system and by the duration of the program which is scheduled to be completed by December, 1962.

1. Reactor Operation

a. Hydrodynamic Studies - A series of high power tests were performed in the EBWR at power levels up to 60 Mwt. Data recorded included recirculation flow rates, void fractions in the downcomer and riser, true interface height in the vessel, subcooling, and vapor carryunder.

The measured amount of subcooling in the water at the inlet to the core reached a peak of 2.6°F at 40 Mw and then dropped with increasing power. At 60 Mw the subcooling decreased to 1.25°F. The calculations based upon the measured flow rates without carryunder indicated that the subcooling should amount to 8.75°F at 60 Mw.

The vapor carryunder occurring in the reactor was calculated from a heat balance utilizing the measured subcooling and flow rates. The amount of carryunder of steam in the recirculating water in the downcomer remained fairly constant as the power was increased and was of the order of 24% by weight at 40 Mw. Above 40 Mw the carryunder began to

increase. At 60 Mw the data indicated that 32% of all the steam generated in the core was carried under. Complete loss of subcooling was estimated to occur with 34.6% carryunder.

b. Power Coefficient Measurements in EBWR Up to 60-MW Power Levels - The power coefficients of $\Delta k/\Delta$ (Mw) $\simeq$0.065%/Mw was reported in ANL-6610 (Progress Report for August, 1962) for power levels from 10 Mw to 40 Mw.

Operation of the reactor in the 40 Mw to 60 Mw range, however, resulted in an increase in the power coefficient to $\simeq$0.1%/Mw. The excess reactivity in the void fractions at 60 Mw operation was 5%, and corresponds to an average steam void fraction in the core of about 20%; the latter amount was that calculated for the average void fraction at 100 Mw. The calculations indicate that for zero carryunder at 60 Mw operation, the void fraction should be 15% and require 3.75% excess reactivity.

Assuming that these reactivity losses result from the excess steam voids in the core, it will be necessary to add additional reactivity to achieve higher power. Additional reactivity is achieved by removing boron strips from the spiked elements. The number of strips that can be removed, however, is subject to the eight- and nine-rod shutdown requirements stated in the hazards report (eight-rod shutdown with boric acid and nine-rod shutdown without the boric acid).

c. EBWR Transfer Functions - The most recent transfer function measurements made on the EBWR were performed under the following operating conditions:

(1) 40 Mw, equilibrium xenon, 600 psig, with a boric acid concentration of 2.73 gm/gal. Control rods Nos. 1 through 8 at 48 in. and center rods at 30 in.

(2) 60 Mw, equilibrium xenon, 600 psig, with a boric acid concentration of 0.46 gm/gal. Control rods Nos. 1 through 8 at 48 in. and center rod at 30 in.

The measurements were made using the rod oscillator at 32 different frequencies ranging from 0.0012 to 9 cps. Data were recorded with the null analyzer, analog sine-cosine cross-correlator and digital data system. Analog recordings were made of noise and transient response. Root mean square (rms) noise was measured using an analog computer. The auto-correlation function and power density spectrum were calculated from the digital noise recordings. Flux signals from two in-core ionization chambers, when compared with the out-of-core chamber, showed an additional two-degree phase lag from the in-core measurements at 56 radians/sec. The conclusions resulting from the extrapolation of the data predict stable operation of the reactor up to 85 Mw of power, providing sufficient excess reactivity can be added.

d. Interface Height - Data on the interface height show that a substantial difference exists between the true water interface level in the reactor and the level indicated by the water column and is caused by the presence of steam voids in the reactor. A linear extrapolation of the data from 60 Mw to 100 Mw indicates that the differential height would be about $4\frac{1}{2}$ ft. Should the interface height continue to rise at the present level, serious carryover problems may occur at the very high power levels.

e. Primary Water Leaks in EBWR - Two water leaks have occurred in the hot primary water system of EBWR, resulting in temporary contamination of the plant air by radionuclides emanating from the reactor water. The first leak occurred on July 26, and Na^{24}, Mn^{56}, Mn^{54}, Co^{58}, and Co^{60} were detected in the air-filter monitors in the plant. The water leak occurred in a welded joint in the reactor water level sight gauge and has been repaired.

The second leak occurred during the September 8-12 period and released the same radionuclides, plus a 9.5-minute half-life Mg^{27} isotope. The presence of this 9.5-minute half-life isotope indicated that the leak was in a flowing (non-stagnant) portion of the primary water system. The leak was traced to a sample valve located on the main floor and it was repaired.

B. BORAX-V

1. Operations and Experiments

High-temperature, pre-operational tests were completed; and high-temperature zero power tests on the boiling core were begun. The zero power tests were interrupted for the repairs and modifications discussed below.

Tests of the boron addition system showed that, by maintaining the boron addition tank at the same temperature as the reactor vessel, the system will operate satisfactorily (without excessive steam hammer). The batch feed system modification for heating the tank before adding the water to the reactor was test-operated and found to be satisfactory. The performance of the superheater drain system and of the source drive at pressure was also satisfactory.

The high-pressure-steam safety valves were tested and adjusted for correct operating pressure. The low-pressure safety valves could not be tested because the electric preheat system does not have sufficient capacity to maintain pressure in the low pressure steam system. These valves will be tested during initial power operation.

Deflection of the Belleville spring between the reactor vessel head gussets and core structure, due to differential expansion while heating to

relief valve operating pressure (685 psig, 503°F), was found to be 0.1 in. compared to the calculated 0.143 in. Since this will provide ample hold-down under natural circulation (for which this spring is designed) this deflection will be satisfactory.

The reactor was made critical at 600 psig, 489°F, to measure the reactivity effect of 128 void tubes in the center 16 fuel assemblies. The bank control rod position was 21.03 in. at a boric acid concentration of about 11 g/gal. Gold flux wire irradiations were made in eleven locations along a diagonal and in four additional locations in the core. Flux wires were contained in pressure-tight, $\frac{1}{8}$-in. O.D. x 0.020-in. wall stainless steel tubes. The power during the irradiation is estimated to have been 300-500 kw. The maximum fuel rod center temperature measured was 510°F.

Boiling fuel assemblies were removed from the reactor for the recovery of temporary flux wire holders after the initial hot critical operation and irradiation. It was noted at this time that the twelve $\frac{1}{8}$-in. dia., X-8001 aluminum rivets attaching the stainless steel upper grid to the X-8001 aluminum fuel assembly box had sheared in some of the assemblies. There was no yielding of the holes in the aluminum box. Preliminary microscopic examination of the failed rivets showed no sign of yielding or elongation, but rather a brittle-type failure. Hardness tests on the sheared face of several rivets gave a range from too-soft-to-measure to Rockwell H-95, which corresponds to a H-18 temper. The hardness of annealed X-8001 aluminum is in the range of Rockwell H-45 to H-65.

The calculated shear stress on the rivets at zero power and operating temperature is 3000 psi. The calculated bearing stress on the side of the holes in the $\frac{1}{16}$-in.-thick aluminum box is 4200 psi. ALCOA data (ANL-5927) give a tensile yield strength of 6200 psi at 500°F after 100 hr at temperature. Creep and shear strength data are not available. The reason for the rivet failure is not known, but could possibly be an unexpectedly low creep strength in shear for X-8001 aluminum.

Because this rivet failure possibly permitted the movement of fuel, the results of the reactivity measurements and flux wire irradiations in the initial hot critical operation are of limited value.

Control rods and drives were checked, and control rod drop times were well within the maximum allowable. Failure due to overheating occurred in five combination guide bushing-wipers made of Delrin plastic. These bushings, located in the control rod drive seals, are cooled with seal water which must be carefully controlled since, if an excessive amount of seal water flows up through the control rod drive nozzles into the reactor vessel, severe thermal gradients are caused in the bottom head. After the damaged Delrin bushings were replaced with spares and the flow of the seal water was carefully monitored and controlled,

operation of the control rod drives was satisfactory and temperature gradients in the lower reactor vessel head were acceptable. The seal water differential pressure control system is being modified to damp the oscillations of the control valve at low reactor pressure.

Following the high-temperature irradiation, difficulty was experienced in removing gold flux wires inside cadmium tubing. The cadmium was not oxidized, but had a shiny, very rough surface appearance indicating that temperatures in the cadmium, which may be due to nuclear heating, were near the melting point. Protective coatings for the cadmium tubing or the use of cadmium alloys are being investigated.

During the month, 34 boric acid determinations were performed for BORAX-V operations; 24 were made on reactor vessel samples and 10 on the boron storage tank. Those reactor vessel samples taken during high-temperature runs were analyzed for chloride content. Most of these had a chloride content equal to laboratory-prepared blanks, but eight samples taken had a range of chloride values from 0.05 to 0.13 ppm. The reactor water demineralizer could not be used with boric acid in the reactor water.

Investigation has revealed that the makeup water demineralizer is not producing rated capacity because silica is not being removed during regeneration. Experiments using hot caustic and a 24-hour soak of the resin are in progress in an attempt to remove the silica and restore rated capacity.

2. Modification and Maintenance

The twelve $\frac{1}{8}$-in.-dia. aluminum rivets attaching each stainless steel upper and lower grid to the aluminum boiling fuel assembly boxes are being replaced with twenty $\frac{3}{16}$-in.-dia. "A"-nickel rivets. This new design gives a calculated shear stress in each rivet of 800 psi and a compressive bearing stress on the side of the holes in the aluminum box of 1400 psi. Riveting and drilling fixtures, rivets, special tools, etc., have been made; and, at month's end, 50 boiling fuel assembly boxes had been modified.

The upper fuel grid on instrumented boiling fuel assembly No. 1-2 was found to have sheared its rivets, and partial disassembly of the fuel assembly was started to allow replacement of rivets. The inlet flowmeter on this assembly has so far defied removal, apparently because of corrosion product buildup between the flowmeter body and the inlet nozzle.

The four control rod extension shafts which were scratched when the Delrin guide bushings failed will be replated; they are being replaced with four new spare shafts. New guide bushings made of Teflon backed with stainless steel, of a design previously used by EBWR, have been

fabricated and installed in the seal housings. These will replace those made of Delrin. Seal water thermocouples have been relocated from the seal leak-off line to the upper seal cavity, in order to monitor more accurately the temperature of the guide bushing.

The bellows in the oscillator rod driveshaft rotating seal failed at high temperature, due to a faulty weld. The bellows was returned to the manufacturer, but repair was not possible and a new bellows was fabricated. A routine metallurgical examination showed improper heat-treatment of the new bellows, which is now being heat-treated again.

Control rods No. 1 and No. 5 were removed for routine inspection and were found to be satisfactory. The control rod channels in the core shroud were also gauged. A 0.475-in.-thick gauge block was successfully inserted in all channels.

3. Analysis

A theoretical model of the BORAX-V reactor and associated systems has been derived. The linearized power feedback paths include the following phenomena: (1) reactor pressure buildup; (2) subcooling of the recirculating water at the core inlet; (3) steam system dynamics, including reactor pressure and turbine inlet pressure control systems; (4) feedwater flow-rate dynamics, including the reactor feedwater level, three-element control system; (5) void reactivity dynamics in the core due to void formation by heat transfer, pressure, subcooling, and recirculation flow rate changes; and (6) Doppler reactivity dynamics due to changes in the average boiler fuel temperature.

The major assumptions made in the analysis are: (1) that the reactor kinetics and all power feedbacks are linear; (2) that the power distribution in the core is space-independent and can be represented in the axial direction by a chopped cosine wave; (3) that the axial void distribution is first-power flux weighted for determination of the effective void volume changes (void reactivity importance function is assumed proportional to the axial power distribution); (4) that the over-all boiler heat transfer coefficient in the subcooled region of the core is the same as that in the boiling region; and (5) that the moderator temperature reactivity changes can be neglected.

The reactor model will be used primarily to: (1) determine analytical power transfer functions ($\delta n/n_0 \delta k_{ex}$) as a function of reactor power level for various combinations of natural vs forced circulation, and boiler vs boiler plus central superheater configurations; and (2) to determine approximate optimized settings for the main steam-to-atmosphere control valve controller and the turbine steam bypass valve controller. In addition, the effect of large input reactivity amplitudes on the reactor

response (describing function) due to the inherent non-linearity in the neutron kinetics may be evaluated with the aid of the "High Power Reactor Describing Function Program," by L. E. Reese and A. A. Wasserman.[1]

4. Critical Experiments

The program of measurements in a critical assembly (ZPR-VII) composed of a central zone of the BORAX-V superheat elements surrounded by a lattice of Hi-C fuel has been completed. The final measurements included uranium foil activation in the voided superheater and the peripheral boiling zone regions. Cadmium ratios and relative activations were also determined with gold, copper, dysprosium, indium, lutetium, and manganese foils at thirteen locations. The data will be used to estimate power distribution, spectral changes, and flux levels in various parts of the core.

The core has been removed from the ZPR-VII system and the superheater elements are undergoing final modifications and assembly required for installation in the BORAX-V reactor.

5. Procurement and Fabrication

a. Superheater Fuel - Brazing and welding of 13 central superheater and 14 peripheral superheater fuel subassemblies has been completed. In addition, the vacuum brazing operation, using Coast Metals-60 alloy, has been finished on six standard fuel elements and one thermocouple element for the instrumented central superheater fuel assemblies. Attachment of risers and nozzles to the central superheater fuel subassemblies was started, and one fuel assembly was completed.

Inspection of the 26 superheater fuel plates furnished by Atomics International as replacements for previously rejected plates has been completed, and all plates except one were found acceptable.

b. Experimental Components - Development work on the brazing of fuel plate thermocouples into sample superheater fuel plates has continued, and Coast Metals-60 alloy appears to give the most satisfactory joint. The problem of voids between the thermocouple tip and bottom of the slot in the edge of fuel plates has been solved by the addition of a small quantity of stainless steel filings to the brazing compound. Other brazing materials were not as satisfactory in eliminating this problem.

Modifications to the recombiner test rig are continuing. Knall-gas flow-measuring equipment, using thermistors, was tried, but proved to be quite unstable and has been discarded. A system design for generating Knall-gas using relatively pure water has been received from General Electric Company and is being considered for adaptation to the recombiner equipment.

---

[1] IDO-16755, Appendix A-3.

The low-water-level cutout on the recombiner was modified to fail safe. A separate fail-safe device, which cuts out the heaters upon sensing high boiler wall temperature, has been ordered. This device uses thermocouples and will be provided with thermocouple burnout protection.

6. Design

Detailed design and checking of the "head-on" boiling fuel assembly handling tool to reload assemblies through nozzles in the reactor vessel head has been completed. Design of the boiling fuel rod manipulator and traversing mechanism for the gamma-scanner, and design of a special oscillator rod fuel assembly containing a stator of 2 w/o boron-stainless steel in a 165° arc, $\frac{1}{8}$ in. thick with three fuel rods in each corner, have also been finished. After test-fitting in the core, the design of the $\frac{3}{8}$-in.-dia. pressure thimbles for miniature ion chambers was modified.

It has been decided that the previous design of a step-function generator, consisting of a slug of poison operating in a Zircaloy-2 pressure thimble, had inadequate reactivity worth to accomplish a satisfactory reactor "ringing" experiment. Therefore, a new combination control rod drive/step-function generator mechanism is being designed to actuate an intermediate control rod.

7. Development and Testing

a. Advanced Superheater Fuel - AISI Type 406 stainless steel is being considered for test of superheat fuel elements in BORAX-V. Atomics International, which fabricated the initial superheat core, has conducted a program to demonstrate the feasibility of fabricating cermet type fuel plates using this type steel. Depleted plates of the half-central and full-central types were fabricated and evaluated. From the results obtained, it appears that these plates can be fabricated to meet the specifications pertaining to core and plate dimensions, flatness, squareness, oxide agglomeration, oxide stringering, and core homogeneity.

Two requirements of the specifications were not satisfied by the plates fabricated. Finished plates were covered with a uniform, tightly adherent, blue-grey scale. Either the formation of the scale must be prevented in some way, or a descaling process would need to be introduced to provide clean plates as specified. The greatest cause for concern, however, is the large number of inclusions which were found throughout the plate cores and, in a continuous line, at the clad-to-clad interfaces. If these plates are to be used in reactor elements, the effects of these inclusions will first have to be determined. However, revised fabrication processes may eliminate or prevent their formation.

Clad core and end cladding samples from these fuel plates have been corrosion tested in ambient distilled water and 650°C, 600 psi degassed steam for three days. Reddish-brown corrosion stains appeared on the surfaces of the samples in room temperature water. The plates had been grit-blasted with chilled iron shot between hot and cold rolling, and some particles of grit were apparently embedded in the plate surfaces. The samples in steam were not significantly attacked.

Brazing development work on Type 406 stainless steel samples continues. Thus far, metallographic examinations indicate that vacuum brazing of de-scaled samples plated with 0.0002-in. thickness of nickel and using either Coast Metals-60 or Premabraze-128 alloys is satisfactory. Specimens using these alloys are being prepared for corrosion tests.

II. LIQUID METAL COOLED REACTORS

A. General Research and Development

1. ZPR-III

a. Assembly 41 - Experiments are under way on Assembly 41, a dilute metal core system in which the U^{238} to U^{235} ratio is about 5 to 1. Other core diluents are aluminum and steel, and the radial and axial blankets consist of high-density, depleted uranium. The program of studies with this assembly includes experiments in basic physics and with different radial and axial blankets.

In the core, a four-drawer sequence, containing five columns of enriched (93.2%) uranium, is used to obtain the desired fuel concentration. The diluents in the four drawers are 23 columns depleted uranium, 32 columns 45% aluminum, and 4 columns steel. The core length was set at 32 in.; and, in the initial loading, fuel was loaded into drawers out to a radius giving about 36% of the expected critical loading. The remaining outer radial drawers in the expected core volume were loaded as core drawers, but with aluminum columns replacing the enriched uranium columns. Criticality was approached by increasing the core volume radially in stepwise substitution of enriched for aluminum columns.

At a total loading of 493.8 kg U^{235}, the reactor, with all rods in, was supercritical by 61.2 Ih. With a measured worth of fuel at the core edge of 18 Ih/kg, the just-critical mass would be 490.4 kg U^{235}; and using the final composition, the critical volume would be 439 liters. With this composition, a DSN calculation with empirical corrections gave a critical mass estimate of about 505 kg. Dimensions and compositions of the critical loading are given in Table I.

Central reactivity coefficients were measured for numerous fissionable and nonfissionable materials. Beside determining reactivity effects of usual fast reactor construction materials, the effects of materials with high neutron capture or scattering properties were determined. Some sample-size investigations were made, but with no conclusive results. Table II lists the materials which were placed at the core center and the reactivity coefficients obtained.

Measurements of fission ratios at the core center are in progress. Some new natural and enriched uranium foils had been prepared for the gas-flow absolute fission chambers, and these have been compared with older foils. Agreement of count ratios with plating mass ratios is good. Foils are presently being prepared with U^{233} and U^{234} platings, and these will be compared with platings in the Kirn counters.

Table I. Assembly 41, Loading No. 16

Excess reactivity with all rods in, 61.2 Ih.

Dimensions:

Core:	Length	32.1 in.
	Average Diameter	32.9 in.
	L/D	0.975
	Volume	442 liters
Axial Blanket Thickness:		12 in.
Radial Blanket Thickness:		12.6 in.

Composition:

Core Loading: 493.8 kg U^{235}

Volume %	Core	Blankets
U^{235}	5.96	0.17
U^{238}	29.1	83.4
Type 304 Stainless Steel	14.1	9.0
Aluminum	17.9	-
Void	32.9	7.4

Table II. Central Reactivity Coefficients in Assembly 41

Material or Isotope	Worth (Ih/g mole)	Material	Worth (Ih/g mole)
U^{235}	28.8	Hg	-1.08
U^{238}	-1.29	Mo	-0.95
U^{233}	52.5	Na	-0.06
Pu^{239}	50.3	Nb	-1.42
Ag	-4.26	Ni	-0.38
Al	-0.12	Ru	-1.98
As	-1.91	S	-0.62
B^{10}	-18.2	Sn	-0.80
Ba	-0.13	Steel (Type 304)	-0.27
Be	+0.18	Ta	-4.27
Bi	-0.28	Th	-2.74
C	+0.02	V	-0.09
CH_2	+10.2	W	-1.84
Cr	-0.21	Y	-0.35
Fe	-0.24	Zr	-0.36
Hf	-3.30		

b. Measurements of the Response Time of the Period Meters - Because of statistical fluctuations at the low current levels of the period meters used in ZPR-III, some damping is required to smooth out normal statistical noise in the frequency range greater than about 2 cps. It has always been calculated that the period meters would respond in a shorter period of time if sufficiently overdriven; no experimental verification had been made of this until last month.

The period channel consists of a $B^{10}F_3$-filled ion chamber, logarithmic preamplifier, differentiating and post-amplifying circuit, indicating meters, and trip circuit, ending in either of two alternate relays in the main scram circuit of the reactor. One of these relays is set to trip at 15 sec and the other at 5 sec.

The circuitry from the logarithmic preamplifier, to and including these relays, is identified as Model No. CD-71. The time required to trip the entire CD-71 circuit was measured with an exponential generator for input periods of 15 to 0.10 sec. Then, step functions of various magnitudes were used to study even shorter response times. The measurements were made with a wide range of starting steady currents, I_0.

The CD-71 was first calibrated, as in actual operation, using the internal (static) calibration. The static current level indicated as input was then calibrated against an external current source believed to be accurate within a few percent, with results shown below:

Period Meter Current Indication	Current Source
1.5×10^{-12}	1×10^{-12}
1.1×10^{-11}	1×10^{-11}
1.0×10^{-10}	1×10^{-10}
0.8×10^{-9}	1×10^{-9}
0.7×10^{-8}	1×10^{-8}
0.55×10^{-7}	1×10^{-7}
0.45×10^{-6}	1×10^{-6}

The e-folding time measured on the logarithmic current circuit of the CD-71, before differentiation, was found to be accurate to within $\pm 10\%$ over the range 0.10 to 15 sec. The slower periods were timed using a stop watch and the faster ones with an oscilloscope. In each case, an accurate exponential signal generator supplied the input.

To measure the trip time, a steady starting current, I_0, was applied at the input to the logarithmic preamplifier of the CD-71, and at time t_0 the input current was caused to start increasing exponentially using

an exponential generator. Time was measured from t_0 until the relay output of the CD-71 chassis had tripped. These times are recorded in Table III for the 15-sec relay and in Table IV for the 5-sec relay. It is encouraging to note that, even with periods as short as 0.10 sec, the 15-sec trip responded before two e-foldings.

Table III. 15-Second Trip Time

Starting Current, I_0, amps	Period (sec)				
	15.1	4.62	1.87	0.49	0.10
10^{-12}	10.3	2.35	1.09	0.452	0.197
10^{-11}	4.62	1.42	0.793	0.397	0.185
10^{-10}	3.16	0.937	0.533	0.296	0.160
10^{-9}	2.39	0.773	0.436	0.241	0.134
10^{-8}	1.82	0.664	0.383	0.217	0.122
10^{-7}	1.40	0.564	0.339	0.198	0.115
10^{-6}	1.03	0.467	0.289	0.176	0.106

Table IV. 5-Second Trip Time

Starting Current, I_0, amps	Period (sec)			
	4.62	1.87	0.49	0.10
10^{-12}	5.33	2.06	0.688	0.232
10^{-11}	3.50	1.41	0.574	0.218
10^{-10}	2.89	1.01	0.421	0.183
10^{-9}	2.30	0.851	0.356	0.157
10^{-8}	1.78	0.725	0.314	0.144
10^{-7}	1.37	0.605	0.278	0.133
10^{-6}	1.05	0.482	0.236	0.119

The time response to a step increase in current was also measured. This is, of course, a function of the magnitude of the step as well as the operating level of the instrument. Therefore, the measurement was made by applying a steady state starting current, I_0, altering this within a microsecond to a new value I_1, and measuring the time until the relays tripped. The results are given in Tables V and VI, for the 15- and 5-sec trips, respectively. The delay required for opening the relay on the CD-71 chassis is about 10 msec, which is included in the times listed in Tables III through VI.

Table V. 15-Second Trip Time from Step Change

I_0 amps	I_1 (amps) 10^{-10}	10^{-9}	10^{-8}	10^{-7}	10^{-6}	10^{-5}	10^{-4}
10^{-12}	0.145	0.076	0.053	0.044	0.041	0.043	0.040
10^{-10}	-	0.086	0.056	0.047	0.044	0.043	0.041
10^{-8}	-	-	-	0.063	0.051	0.047	0.043

Table VI. 5-Second Trip Time from Step Change

I_0 amps	I_1 (amps) 10^{-10}	10^{-9}	10^{-8}	10^{-7}	10^{-6}	10^{-5}	10^{-4}
10^{-12}	0.183	0.072	0.042	0.033	0.032	0.031	0.030
10^{-10}	-	0.087	0.051	0.037	0.034	0.031	0.030
10^{-8}	-	-	-	0.064	0.044	0.036	0.034

It should be noted that, in actual operation of a reactor scram, the CD-71 relay is followed by another relay which requires about 15 msec to operate; and this is what actually opens the dc circuits to the rod clutch magnets. The time required from interruption of dc to initial movement (1-in. travel) of the rods has been measured to be about 27 msec; and the subsequent time for the next 8 in. of rod travel is generally about 125 msec.

2. ZPR-VI

a. Building - The installation of all major components for the ZPR-VI facility has been completed. The control wiring including the interlock circuitry has been checked and been found to be satisfactory. The modifications to the control wiring for the reactor cell ventilation system are expected to be completed by October 15. The installation of the argon gas storage system for use in the event of a uranium fire will be accomplished by the end of October.

b. Assembly - All of the ten required dual-purpose control/safety rod drive mechanisms have been tested and installed on the facility. Minor modifications on the insertion safety rods, which will be used with large dilute cores, are in progress. These modifications will be completed by October 31.

The deflection measurements being made on loaded matrix tubes in the assembly, which is logically a part of the experimental program, are continuing. These data will be used to improve the accuracy of the results to the experimental program.

Based upon the current schedule, loading of the facility for the investigation of an all metal core similar in composition to Assembly 22 of ZPR-III could commence about the first of November subject to prior receipt of approval of the Hazards Summary Report.

All of the enriched uranium fuel, depleted uranium, stainless steel, and other mockup elements are on hand to conduct the experiment.

3. AFSR

Work is continuing on the criticality meter. The equipment is complete and installed at the beam hole. Plans are to oscillate a 2-in. diameter x $1\frac{1}{2}$-in. cylinder of steel through a $\frac{3}{4}$-in. stroke at the inner end of the beam hole. This is expected to give a peak-to-peak reactivity effect of about 40 Ih, based on static reactivity measurements made previously. Meanwhile, the electronics are being tested with a simulated neutron chamber signal. As a preliminary to actual testing of the reactivity meter, the reactivity effect of the plug position has been measured.

The detection of neutrons in the presence of gamma by means of color discrimination is being investigated, and a number of scintillator materials now on order will be delivered next month.

Results on the interlaboratory comparison of foil-counting techniques have been received from the participants (Argonne, Los Alamos, and Hanford), except that Hanford still required one normalization of counters which is to be supplied shortly.

Work on the AFSR plant this month includes fabrication of a new gamma monitoring system (which should be installed in two or three weeks) and installation of additional limit switches on the safety rod drives. These switches facilitate obtaining unambiguous rod drop times. Present indications are that actual rod drop times are somewhat better than those indicated in the hazards report.

B. EBR-I

1. Mark III Operation and Preparation for Operation on the Mark IV Core

The irradiation of various steel Izod impact specimens and nickel flux wires, carried out in connection with a study of the irradiation damage to materials in a high quality fast flux, was completed.

The CRL Model D manipulators have been installed in the hot cell and it is now ready for use.

A storage rack for the remaining Mark III fuel rods was installed in the EBR-I storage vault, and it is now ready for receipt of Mark IV fuel.

Calibration of new sheathed thermocouples was completed, and those found defective were returned to the vendor for replacement.

2. Core IV Fabrication

a. Production of Blanket and Thermocouple Rods - Eight Zircaloy-2 thermocouple well tubes were completed for assembly of the thermocouple elements for this loading. Since the thermocouple occupied the opening used for NaK filling and level adjustment, it was necessary to load these elements with a measured quantity of NaK before installation of the thermocouple well. After final assembly and closure weld the thermocouple rods were bonded, eddy-current tested and X-rayed.

Bonds were satisfactory on all rods, but X-rays showed only one rod with a satisfactory NaK level. The unsatisfactory NaK levels were readjusted by cutting the filler tube just below the closure weld and removing the thermocouple well. A small quantity of NaK was added or removed, the rods reassembled, welded, bonded and inspected. NaK levels on the second attempt were found to be satisfactory on six of the eight rods assembled.

b. Compatibility of Pu-1.25 w/o Al with Zircaloy-2 - A series of heat treatments is being performed on Pu-1.25 w/o Al vs Zr-2 diffusion couples to determine the degree of solid interaction between the fuel and cladding of the EBR-I Mark IV loading. Temperatures from 500°C to 650°C for up to six weeks are included in the study. Shorter time specimens are now being examined metallographically and the heat treatments are being continued.

c. Breeding Gain Specimens - The Zircaloy tubing and hardware were received for the four special Mark IV and special Mark III type breeding gain rods. These rods were assembled, filled with NaK, welded closed, and bonded using the technique developed for the Mark IV core. Although the eddy-current traces were difficult to interpret because of the large number of specimens in this rod, the bonding appeared to be acceptable. Sodium levels were acceptable. The rods were leak tested and found tight.

C. EBR-II

1. Reactor Plant

a. Rotating Plugs - In the Report for August, 1962 (ANL-6610) a complete description of the rotating plug freeze seal difficulty was given, including the plans for correction.

The large plug seal trough lower insulator plate has been installed, welded and leak tested. The thermocouple support ring has been

positioned and welded. The low flow purge gas lines, thermocouple tubes and tube clips were installed. The spring segments that form the seal with the "J" ring and permit radial and vertical movement of the large trough and retainer strips have been installed. The large trough cut off inner wall was lowered and positioned and is ready for welding.

The secondary seal spring components are being installed on both rotating plugs. The solid stainless rings have been installed and welded to the existing dip rings on both plugs. The drilling and reaming of the heater holes in the new ring has been completed on the large plug. The leak testing of the welds is completed. The heater hole drilling and reaming in the small plug is in progress. The outside window holes in both plugs have been completed. The inside window hole on the large plug is being drilled at the present time. The installation and rework of all the dampers in the large plug have been completed. The damper actuating shaft holes have been drilled and reamed in the small plug, and the installation of the dampers should start shortly. The wire-way to house the large plug heater leads is just about completed. The inner grease retainer and lower race packing ring has been positioned and installed on both plug bearings.

b. Transfer Arm Mechanism Modification - The transfer arm mechanism is part of the fuel handling system and provides the means for transferring fuel subassemblies between the gripper mechanism, the storage rack, and the transfer port. A view of the mechanism prior to modification is shown in ANL-6544 (Progress Report for March, 1962).

As part of the future development program, it was planned to modify the transfer arm mechanism by incorporating a vertical movement of approximately 12 in. which would give the transfer arm operator additional "feel" during the fuel handling sequence. Because of the delay in filling the primary tank with sodium occasioned by the rotating plug seal difficulties, it was decided to carry out the transfer arm modifications concurrently with the rotating plug revisions rather than wait for a later date. These modifications will not cause any delay in the reactor construction schedule and will make it possible to operate the modified transfer arm mechanism during the dry fuel handling system checkout.

Figure 1 shows the modified design of the transfer arm mechanism. The principal changes consist of a new transfer arm suspension and counterweight for the 12 in. vertical movement and a counter-balance for the horizontal part of the transfer arm to assure more balanced loads on the vertical shaft.

The new transfer arm suspension provides for a counterweight of approximately 1700 lb which is connected with a chain to the movable part of the transfer arm mechanism. The chain is stretched across sprockets which are mounted on a T-shaped support structure. Thus,

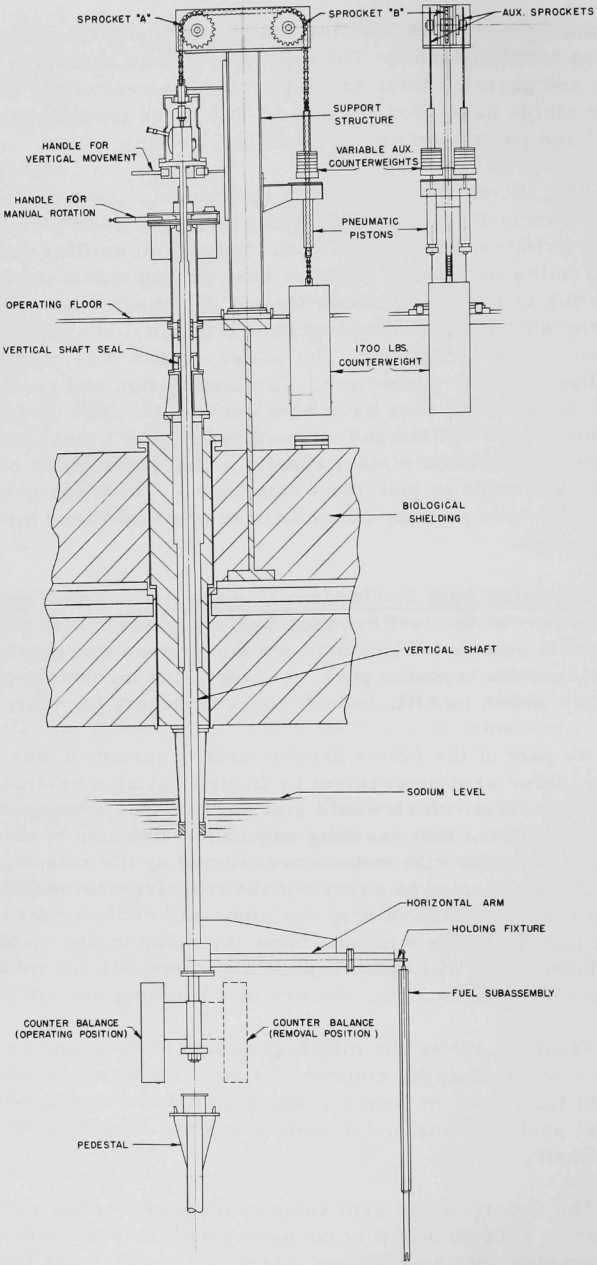

Figure 1. Modified Transfer Arm Mechanism

when the operator raises the transfer arm, the counterweight moves downward requiring only enough force by the operator to overcome the friction of the system. Since the transfer arm weight will vary depending on whether it is empty or supporting one of several types of fuel subassembly, two auxiliary counterweights, variable between 10 to 140 lb, can be added at the proper time in each fuel handling sequence.

The transfer arm mechanism has been shipped to the DuPage site for rework. Several sections of the vertical shaft have been refabricated. The vertical shaft seal components, the horizontal arm counter balance, and the pedestal have been completed. A 20-ft support structure has been adapted to serve as a preassembly facility.

2. Power Plant

All fan stacks were reinforced and ample fan tip clearance is now assured. Repair to the fan stack linings has been completed. Structural bolts throughout the tower have been tightened. The cooling tower basin was drained and cleaned while modifications were being made to plant cooling water piping in other parts of the facility. Installation of an 8-in. bypass line around the gate valve on the discharge side of condenser circulating pump No. 2 is now in progress. This will permit reduced circulation rates during cold weather operation of the cooling tower. Miscellaneous modifications and additions were made to gauges and drains associated with the turbine.

3. Sodium Boiler Plant

Work continued on the following items: (1) fabrication and installation of flashing around piping and equipment; (2) insulating of piping and equipment; (3) installation of heater wire and thermocouples and their related wiring; (4) painting of pipe and coating of miscellaneous ferrous surfaces and structural steel; and (5) removal of all scaffolding from the upper portions of the boiler wing of the building.

4. Fuel Cycle Facility

a. Construction and Installation - Testing of the capacity and balancing of the Fuel Cycle Facility heating and ventilating system was undertaken. Total air supply volume was found to be approximately equal to the design value, but the air distribution was incorrect in some areas. In adjusting dampers to correct this, it was found that they were poorly fitted and modifications are required.

The drying system for the argon cell atmosphere was placed in operation, and reasonable rates of water removal were attained to dewpoints in the vicinity of +30-40°F. However, in regenerating the molecular

sieve drying agent with hot air, the desired regenerant temperature of 660°F could not be achieved. Improper operation of freon expansion valves in the argon cooling system presented further difficulty.

The failure of the bridge drive gear reducer unit on one of the Argon Cell cranes is being attributed to the starting torque of the motor, which exceeds the rated torque of the gear reducer unit. The gear reducer unit, which drives a large mass of equipment, may have failed because of being subjected to the full starting torque of the motor. Replacement motors with suitable starting torques are being investigated.

The compressors for recirculating the Argon Cell atmosphere are being installed on the service floor outside the subcells. An isolation wall has been erected around the compressor area, and a separate ventilation system for this area will be installed.

The design of the Fuel Transfer Coffin, which is being fabricated at Argonne, is nearly complete. Fabrication of component parts has been started. The vendor-supplied coffin is being given preliminary tests at the vendor's shops.

The final inspection of all Fuel Cycle Facility shielding window units has been done. The light transmittance of the windows, tested with a light color temperature 2848°K, was determined to be from 15 to 17 percent, which exceeds the guarantee of 9 percent. General viewing quality is excellent.

Wide angle optical viewers located in the roof of the Argon Cell will make it possible to view the interior of the cell from above. Three of the four viewers planned have been installed.

The Argon Cell manipulators have performed satisfactorily when used for the remote installation of cell equipment.

Two injection casting furnaces have been installed by remote methods in the Argon Cell. These furnaces recast into fuel pins the purified metal ingots received from the melt refining furnaces.

It is planned to evaluate the integrity of the air and argon cell shielding walls by placing intense gamma sources at various locations inside the cells and surveying the cell's exterior with scintillation probes. Arrangements have been made for irradiation of capsules of sodium at the MTR to provide approximately 5000-curie sources of sodium-24 to make the shielding survey about the end of October.

b. Development of Remote Control Methods and Equipment for Fuel Fabrication - The fuel pin processing machines, settling machines, sodium bonders and leak detectors for in-cell installation have been

delivered by the vendors. These machines are being tested at Argonne, Illinois with their ANL-fabricated control components prior to shipment to the NRTS.

The fuel pin process machines were functionally inspected at Combustion Engineering, Inc. where major components were made interchangeable and the piping tested for leakage. In the short time, and with the limited number of castings available, it was not possible to tune this equipment so that it would work on a moving stream of fuel castings nor to perform the necessary reliability tests.

Finely lapped surfaces were used to seal the valves in the pressure type leak detector heads. While these seals functioned satisfactorily on the prototype leak detector, they were not tight on the production leak detectors. Lead and aluminum gasket washers were tried but these extruded under the high pressures required. A silver plated sealing surface was found to be satisfactory on the valves and the four additional leak detector valves are now being silver plated.

The drive and control circuits for the bonding and settling machines were designed, constructed and operated successfully. The machines are being modified to incorporate the actuator switches required for operation.

The air cell piping drawings, electrical schematics and interconnection diagrams for leak detectors, bonders, bond testers and fuel element assembly machine were completed during September.

c. Fuel Element Decanner for the Fuel Cycle Facility - The principal mechanical subassembly of the Fuel Element Decanner, the spiral decanning unit, has been modified to improve its reliability. Testing had indicated that the spiral decanner did not always have sufficient driving force to start a cut when the sheared end of the stainless steel tubing was flared over the end of the fuel. With the modified unit, the force on the drive rolls and the cutting tool is increased during the instant that the cut is started and is then reduced to allow for variations in the diameter of the fuel elements. The rigidity of the tool holder has also been increased. The modified decanner has decanned 400 elements with varying degrees of tubing flare-over and has repeatedly cut through these tubing ends, including those that were completely closed over the fuel.

d. Development Studies - Development studies continued on the distillation of magnesium-zinc in the melt refining furnace (see Progress Report, July 1962, ANL-6597, page 21). In a run in which 1,000 grams of 50 percent magnesium-zinc was distilled from the graphite crucible, 81 percent of the charge was collected in the graphite collector, 6.9 percent was collected in the graphite condenser, 9.6 percent was collected on

the Fiberfrax insulator, and 2.5 percent remained in the crucible. No magnesium-zinc was noted on the interior surfaces of the furnace. The collector had to be tapped slightly before separating it from the crucible at the end of the run. A few small beads of metal caused this bonding between the two pieces. Modifications in the design of the condenser unit are planned to overcome this problem.

To determine what happens to rare earth fission products in melt refining and related processes, analyses are usually made for cerium as an indicator of rare earth behavior. To provide a means for confirming that behavior of rare earths is consistent, analytical methods have been developed for determination of several individual rare earths at very low concentrations in fissium alloy by means of flame photometry.

5. Fuel Development

a. Properties of Uranium-Fissium Alloys - Compatibility studies are being made to determine the interaction by solid diffusion between the fuels and cladding of the Mark I loading in EBR-II.

Heat treatments have been performed at 550°C, 600°C, and 650°C for one, two and five weeks, and at 700°C for five weeks on diffusion couples of uranium-5 w/o fissium alloys with Type 304 stainless steel. All the heat treatments have been finished and the specimens have been inspected metallographically.

Good bonding was observed on all couples and measurements of the total width of the diffusion band are given in Table VII. Only about 5 percent of the diffusion penetration is into the stainless steel. The balance of penetration is into the uranium-5 w/o fissium alloy.

Table VII. Total Diffusion Band Widths (mils) Between Uranium-5 w/o Fissium and 304 Stainless Steel

Temp (°C)	Band Width (mils)		
	1 wk Anneal	2 wk Anneal	5 wk Anneal
550	0.75	1.0	1.65
600	1.75	2.3	3.75
650	3.9	5.3	8.5
700	-	-	21.0

b. Fast Reactor Fuel Jacket Development - Further examination and evaluation of the niobium alloy tubes (see Progress Report, July 1962, ANL-6597) received from the Wolverine Tube Co. has led to the conclusion that these tubes are not suitable for reactor use. Eddy-current

inspection indicated that only 30-50 percent of the wall thickness was free of defects. This tubing is to be replaced and until the new tubing is received no further evaluation of these alloys (Nb-5 w/o Zr and Nb-5 w/o Zr-10 w/o Ti) will be made.

Thirty-three feet of molybdenum tubing of random lengths measuring 0.156 in. I.D. x 0.003 in. wall have been obtained for the purpose of fabricating duplex tubing. Evaluation of the tubing by eddy-current inspection indicates that all the tubes contain numerous defects penetrating at least 30 percent of the wall thickness. Work is in progress on the duplex tube, which will consist of the molybdenum tube bonded to an exterior tube of Type 304 stainless steel or a nickel base alloy. One of the main problems will be to avoid propagation of the existing defects; otherwise the material will have limited usefulness even for process evaluation and irradiation test purposes.

6. Process Development

a. Melt Refining Process Technology - An investigation was completed on the behavior of iodine during off-gas handling operations following melt refining of highly irradiated EBR-II fuel. The gases released during melt refining are to be pumped to an exterior storage tank, from which they are to be disposed of through a stack when meteorological conditions are favorable. Since iodine has been noted to deposit on copper process lines, it is desirable to remove iodine-131 from the off-gas stream by equipment inside the Argon Cell to prevent process lines in working areas from becoming radioactive. A trap for this purpose consisting of a bed of activated charcoal with an AEC filter at each end of the trap was tested. After an ingot from a high-activity melting experiment (350-gram-uranium scale) was cast, volatile xenon-133, krypton-85, and iodine-131 present in the furnace atmosphere were evacuated through the trap, which removed from the gas stream 250 microcuries of iodine-131. Only one microcurie of iodine-131 appeared in the effluent from the trap during pumpdown. The trap retained iodine well at the 8.5 mm (mercury) pressure existing at the end of furnace pumpdown.

b. Skull Reclamation Process - Work on the demonstration of the skull reclamation process is proceeding on a 130 gram uranium scale in an argon atmosphere. Two noble metal extraction runs, each performed with a salt flux composition (mole ratio) of 47.5 $CaCl_2$, 47.5 $MgCl_2$, 5 MgF_2 plus two percent zinc chloride, gave satisfactory removals of ruthenium. In one of these runs, no water was added to the flux and ruthenium recovery was 90 percent. In the other run, absorption of water to a 0.7 weight percent concentration in the flux was allowed and the ruthenium recovery was 100 percent. These may be compared with a ruthenium recovery of 63 percent for a flux containing one percent zinc chloride and recoveries below 40 percent in the absence of zinc chloride.

The thixotropically cast beryllia crucible which was previously reported (see Progress Report for August 1962, ANL-6610, page 34) to have withstood skull reclamation precipitation and retorting steps of temperatures above 450°C for 184 hours has now withstood these conditions for a total of 375 hours with no visible deterioration. Testing of the crucible will continue in order to establish its useful life.

Alundum crucibles fabricated by pressing are being evaluated as low-cost substitutes for beryllia crucibles in the skull reclamation process. In a 100 gram uranium scale run, an Alundum crucible was subjected to intermetallic precipitation, uranium precipitation, and retorting conditions. Some leakage of molten metal through the porous structure of the crucible wall was noted. The application of ceramic coatings as slips followed by firing, is being investigated as a means of preventing such leakage.

In a separate experiment in which zinc-50 percent magnesium was held at 800°C for 48 hours in an Alundum crucible, there was some seepage of metal into the crucible wall. Although up to 0.1 percent aluminum was introduced into the melt, this does not disqualify alumina as a material for this process, as aluminum can probably be removed in a waste metal stream.

c. Blanket Processing Studies - Four additional runs on a four kilogram uranium scale have been completed as part of a plant-scale demonstration of the phase separation step which follows uranium precipitation in the blanket process. In these runs, magnesium-zinc-uranium charges were stirred at 800°C, magnesium was added to precipitate uranium, and the mixture was cooled to 415° to 475°C prior to transfer of the plutonium-bearing supernatant by pressure siphoning. Techniques and equipment were improved during the course of these runs. The percent separations of supernatant phase were, in order, 90, 94, 99, and 98 percent. A 95 percent phase separation is regarded as adequate.

d. Plutonium Recovery Process - The separation of rare earths from uranium and plutonium by selective extraction into a molten halide flux has been studied further. Distribution coefficients for praseodymium and plutonium between 30 m/o NaCl-20 m/o KCl-50 m/o $MgCl_2$ and 50 w/o zinc-50 w/o magnesium have been determined. It was found that the plutonium-praseodymium separation factor can be increased from 30 to 60 by decreasing the temperature from 850° to 425°C. These separation factors may be compared with plutonium-praseodymium separation factors of 25 and 47 between 50 m/o LiCl-50 m/o $MgCl_2$ and 50 w/o zinc-50 w/o magnesium at 850°C and 620°C.

The use of oxidation-reduction titration to separate zirconium from plutonium-uranium-fissium EBR-II second core fuel was evaluated in an exploratory experiment. A process which would utilize this technique is the following:

(1) Dissolution of EBR-II fuel by zinc chloride oxidation in the presence of an inert molten salt and liquid metal solvent. Noble elements would be either dissolved or precipitated in the metal phase while uranium, plutonium, zirconium, and other elements would be oxidized into the salt phase.

(2) Titration of the oxidized zirconium with magnesium metal to transfer the zirconium into the metal phase for subsequent removal by phase separation.

In the experiment performed, irradiated zirconium (dissolved in cadmium) and uranium-plutonium alloy were converted to chlorides when excess zinc chloride was added to the system, 99% LiCl-KCl eutectic-1% LiF/cadmium. The titration curves obtained upon reduction with magnesium at 550°C indicate that at least one-half percent of the uranium and plutonium would be transferred to the metal phase in a single-stage operation.

e. Reduction of Thorium Dioxide - Additional laboratory-scale experiments have been performed on the reduction of thorium dioxide by zinc-5 w/o magnesium alloy in the presence of a calcium chloride-magnesium chloride-calcium fluoride flux at 800°C. By adjustment of the magnesium chloride concentration in the flux, complete reduction of 7-gram to 70-gram thorium dioxide charges has been achieved at thorium loadings as high as 10 weight percent in the metal phase. The sludge formed upon reduction of thorium dioxide was poured more easily when the magnesium content of the alloy was increased to 10 weight percent, as a greater proportion of the thorium remained in solution.

f. Materials Evaluation - Tungsten and molybdenum-30 weight percent tungsten corrosion specimens subjected to noble metal extraction conditions for 400 or 500 hours underwent no detectable changes in dimension, as was reported in Progress Report for June, 1962, ANL-6580, page 25. Metallographic examination and physical testing of these specimens has now been performed. No significant corrosion of pressed and sintered tungsten or of rolled tungsten specimens was found by metallographic examination, and rupture strength of tungsten specimens was found to be little affected by exposure to noble metal extraction conditions. Pressed and sintered tungsten will probably be the crucible material used in processing the first EBR-II core loading. The molybdenum-30 weight percent tungsten specimens were attacked to a depth of two to eight mils and showed a slight decrease in strength. This alloy is nevertheless considered satisfactory for such applications as agitators and transfer lines.

Further work has been done in the development of materials and techniques for fabricating large crucibles by the method of concrete casting (see Progress Report for August 1962, ANL-6610, page 36). It is

believed that very large ceramic crucibles with good mechanical strength and thermal shock resistance can be fabricated from the mixes which have been developed, but that the porosity of such crucibles would be too high for containment of fluxes. A coating which was applied to small beryllia test specimens as a slip and which was bonded by firing at 1600°C for three hours, satisfactorily prevented the penetration of water and is expected to resist the penetration of salt flux also. The coating is a methyl alcohol suspension of BeO, Al_2O_3, and MgO in the weight ratio, 27.5 to 28.0 to 44.5, to which a two percent solution of polyvinyl alcohol in water is added to improve the plasticity of the suspension.

g. Special Projects - The diffusivity of uranium in liquid aluminum was found to range from 0.6×10^{-5} sq cm/sec at 700°C to 3.1×10^{-5} sq cm/sec at 850°C with estimated accuracies of ±15 percent. No further diffusivity measurements are planned.

D. FARET

The general engineering and physics parameters of an experimental facility to test the characteristics of advanced fast reactors are being examined in detail.

It has been proposed that Doppler coefficient measurements be made in a multi-region core consisting of driver, buffer, and test zones. The test zone is the central region and is surrounded by the buffer and driver regions. The test and buffer zones have the same composition as the core to be investigated. The buffer zone serves to equilibrate the spectrum, while the driver zone furnishes whatever additional reactivity is required to achieve criticality. The temperature of the test zone is changed during the measurement.

Two sizes of driver-buffer systems (DBS) were investigated with one test zone as shown below:

No.	Core Identity	Test Zone Radius (in.)	Buffer Zone Thickness (in.)	Driver Zone Thickness (in.)
1	DBS-I	6	9	15
2	DBS-II	6	6	12

Both reactors used the EBR-II composition for the driver zone with the fuel enrichment ranging from 8% to 12% U^{235}. The test zone and the buffer were made up of the composition and fuel to be tested for the FARET systems. Calculations were done for the following compositions:

Reactor Assembly	Fuel	Ratio, Pu^{239}/U^{238}	Composition, Vol-% Fuel	Sodium	Steel
a	PuC, UC	1:7	30	52	18
b	PuC, UC	1:9	30	52	18
c	PuO_2-UO_2	1:7	32	52	16
d	PuO_2-UO_2	1:9	32	52	16

The magnitude of the Doppler effect on reactivity on heating the test zone from 750°K to 1500°K (fuel temperatures), with the buffer zone kept at 750°K, is shown below:

Reactor Assembly	Core Identity	Change in Reactivity, $\Delta k \Big\vert_{750°K}^{1500°K}$
a	DBS-I	0.000458
b	DBS-I	0.000341
b	DBS-II	0.000345
c	DBS-I	0.000475
d	DBS-I	0.000359

A few calculations on the magnitude of the Doppler effect were also done for heating full-sized cores having the composition of the test zone. The results are:

Reactor Assembly	Change in Reactivity, $\Delta k \Big\vert_{750°K}^{1500°K}$
a	0.003549
b	0.005729
c	0.005724

It is seen that the reactivity changes on heating the 1 foot diameter test zone are of the order of one-tenth of those for heating a full core, the exact ratio depending on the test zone environment. The final calibration must, of course, depend on a critical experiment. The temperature change of 750°K is representative of what it is hoped to achieve.

The results on the power generation in the test zone for a 50-Mw total power for the DB systems are:

Reactor Assembly	Core Identity	Power Density, Average Mw/liter of Core
a	DBS-I	0.057
a	DBS-II	0.062
b	DBS-I	0.032
b	DBS-II	0.042
c	DBS-I	0.037
c	DBS-II	0.044
d	DBS-I	0.023
d	DBS-II	0.032

It is believed that these power densities will be adequate to provide sufficient fuel temperature differences to carry out the proposed tests.

III. GENERAL REACTOR TECHNOLOGY

A. Applied Reactor Physics

1. High Conversion Critical Experiment

The ZPR-VII facility is now being reloaded with a uniform Hi-C core. This will consist of approximately 1,400 stainless steel clad, 3 wt-% enrichment UO_2 fuel elements in a 1.24-cm square lattice. Certain maintenance and minor modifications of the facility are being done simultaneously. These include addition of a heater and a cooler to improve temperature control during both temperature coefficient measurements and normal operation.

The infinite dilution cadmium ratios given in Table VIII have been obtained for the center of the Hi-C 1.14-cm triangular core.

Table VIII. Infinite Dilution Cadmium Ratios

Foil	Cd R	Z	E_{res}, Resonance Energy
Dy	7.4 ± 0.1	(1.12 ± 0.10)	(bound)
In	1.061 ± 0.004	1.04 ± 0.10	1.457 ev
Au	1.061 ± 0.008	0.96 ± 0.13	4.91
Mn	1.57 ± 0.02	0.60 ± 0.04	337
Cu	1.53 ± 0.03	0.60 ± 0.05	580
Lu^{175}	$1.00 \; {}^{+0.03}_{-0.00}$	-	2.61
Lu^{176}	4.0 ± 0.4	-	0.142

The quantity Z is defined by

$$Z = \frac{\int_0^{cd} v_0/v \, \phi(E)dE}{E_{res}\phi(E_{res})} = \frac{RI(Cd\ R - 1)}{\sigma_0} \quad ,$$

where RI is the resonance activation integral, $v_0 = 2200$ m/sec, and σ_0 is the activation cross section for $v = v_0$. If the epicadmium flux is truly $1/E$, then Z for any element with a $1/v$ subcadmium cross section is constant. It is observed, however, that indium and gold, while they agree with each other, differ markedly from manganese and copper. This indicates that the flux per unit lethargy in the 300 to 600-ev region is higher than in the 1.4 to 5-ev region by a factor of $(1.0/0.6) \approx 1.66$. The difference is ascribed to resonance capture by the U^{235} in the fuel.

Interpretation of the dysprosium data is made difficult by the fact that the bound energy level causes substantial deviation from 1/v cross-section behavior at thermal energies.

The cadmium difference for the Lu^{175} was too small to be determined with useful accuracy. The Lu^{176} data are plagued by poor statistics. An effort is being made to locate some lutetium-aluminum alloy with a higher lutetium content.

Work is continuing in an effort to extract the maximum spectral information from the available data, for the BORAX-V cores as well as the Hi-C cores.

2. Theoretical Physics

a. Doppler Effect Calculations for U^{235}-Fueled Critical Assemblies - The operation of critical assemblies which have fissile and fertile material physically separated poses a special problem if a significant Doppler effect is present because of time delay in heat flow from fissile to fertile material. This problem has been examined for a U^{235}-fueled assembly (having a 5:1 U^{238}/U^{235} ratio) corresponding to 30 vol-% UC, 20 vol-% steel, and 50 vol-% sodium.

The evaluation of U^{235} fission and capture cross sections is uncertain because of lack of knowledge of resonance parameters and because of the strong overlapping of the resonances in Doppler broadening. The validity of the one-level formula is also questionable. A start has been made using two different sets of one-level parameters for U^{235} which perhaps illustrate the range of uncertainty. Because of the strong overlapping of resonances at higher energies the approach denoted by Nicholson[1] as "Method A" was used in the energy range down to 1 kev. Nicholson's "Method B" - which corresponds to isolated resonances - was used at lower energies. It is believed that this procedure will overestimate the U^{235} reactivity effect corresponding to a given set of resonance parameters.

Calculation on heating of the U^{235} from 300°K to 2500°K gave a positive reactivity effect of +0.2% k with one set of parameters and +0.1% k with the other. Heating by U^{238} fissions gave a calculated effect slightly less than -0.1% k. A large positive effect from the U^{235} thus seems unlikely.

b. ZPR-III Theoretical Studies - A theoretical design for a two-zone loading for ZPR-III has been undertaken. The objective is to use an enriched outer zone to "drive" a central zone which has the composition of

---

[1] R. B. Nicholson, "The Doppler Effect in Fast Reactors," APDA-139 (1960).

a very large power breeder reactor. The central zone is to have the properties of the breeder reactor over as large a region as possible. A 2000-liter carbide power breeder was chosen as the reference system.

It has been shown to be possible, within the available fuel inventory at ZPR-III, to consider a central zone of 40-cm radius, a depleted uranium filter of 2.0 cm and a driver zone of 8.6 cm thickness. Very satisfactory neutron spectral characteristics are found to exist out to approximately 36 cm. A tentative experimental program has been proposed.

c. Calculation of Energy Yield from Maximum Accidents in a Zoned Zero-Power Reactor - In a continuation of studies of the safety behavior of zero-power reactors during severe accidents, a system having a two-zone core has been examined. The central zone had a composition of a 3000-liter power breeder core and the outer region of the core was more heavily loaded with uranium fuel and acted as a driver. It was found that this system has rather poor shutdown characteristics. This is because initial pressures are generated at the zonal interface and strong negative velocities, as well as positive velocities, of core material occur. The consequence of this behavior is that reactivity is reduced at a much lower rate during the interval of peak energy generation. The total energy generated after the threshold for disassembly pressure occurred was almost five times as large for this accident as it was for a single-zone system of comparable size and for which the same reactivity insertion rate at prompt critical was employed.

In an attempt to reduce the potential yield of an accident for this type of system another two-zone loading was chosen. The only change made was to adjust the relative void fractions of the two zones, which might be considered as replacing low density aluminum plates by sodium cans, to control the relative times during the burst at which the pressure threshold is reached in the central zone and in the driver zone. This design change, for the same initial accident conditions, resulted in a decrease of the integrated energy of the burst above the dissociating pressure threshold by a factor of 2.6 and a decrease in the energy generation before the threshold was reached by a factor of four.

d. Mathematical Numerical Methods Analysis - It is well known in one-dimensional numerical quadrature that it is frequently better to subdivide the range, and to apply a relatively low-order formula, such as the trapezoidal formula or Simpson's rule to each region separately, rather than to attempt to use a higher order formula of the Newton-Cotes or Gaussian type over the entire range. Ralston[1] has described a family

[1] A. Ralston, "A Family of Quadrature Formulas which Achieve High Accuracy in Composite Rules," J. Assoc. Comput. Mach. Vol. 6, pp. 384-394 (July, 1959).

of such formulas in which the values of the function at each end of the interval appear, but with opposite weights, so that when the formulas are compounded, the contributions from the junctions between subintervals cancel. Thus, it is possible to obtain the effect of one additional point in each subinterval (i.e., to use a formula which is accurate for polynomials of one higher degree) at the extra cost of computing the integrand at the two ends of the entire interval only.

In multiple quadratures, the advantages of this device are even greater. For these applications, a family of second-degree formulas have been derived for any number of dimensions which require only one point in the interior of each sub-rectangle, and one point in each face. The points in the faces cancel when the formula is compounded.

In s dimensions, the formula for the hyper-rectangle $\left(r^{(i)}-1\right) h^{(i)} \le x(i) \left(r^{(i)}+1\right) h^{(i)}$ is:

$$\int_V f(\underset{ww}{x})\,d\underset{ww}{x} = \prod_{k=1}^{s} \left(2h^{(k)}\right)\left\{\frac{\sqrt{3}}{6}\sum\left[f\left(\underset{ww}{x}_{2j-1}\right) - f\left(\underset{ww}{x}_{2j}\right)\right] + f\left(\underset{ww}{x}_{2s+1}\right)\right\}$$

where

$$x^{(i)}_{2j-1} = h^{(i)}\left[r^{(i)} + \frac{\sqrt{3}}{6}\left(1-\delta_{ij}\right) - \delta_{ij}\right] ,$$

$$x^{(i)}_{2j} = h^{(i)}\left[r^{(i)} + \frac{\sqrt{3}}{6}\left(1-\delta_{ij}\right) + \delta_{ij}\right]$$

and

$$x^{(i)}_{2s+1} = h^{(i)}\left(r^{(i)} + \frac{\sqrt{3}}{3}\right) .$$

Here δ_{ij} is the Kronecker delta, superscripts refer to the components of the vectors $\underset{ww}{x}$, $\underset{ww}{r}$ and $\underset{ww}{h}$, while subscripts refer to particular points.

The two and three-dimensional formulas may be used not only in strict numerical applications, but also in the design of experiments to estimate the integral of physical quantities such as flux through a rectangular fuel element.

B. Reactor Fuels Development

1. Corrosion Studies

a. Zirconium Alloys for Superheated Steam

(1) Tests in Deoxygenated Steam at 540°C, 600 psi - Five samples of a group of ANL experimental alloys have survived 52 days' exposure to these test conditions. The resistant samples contain 1-3 w/o copper and iron additions and confirm earlier results.

Samples of Zr-Ni-Fe and Zr-Cu-Fe ternaries manufactured for ANL by Carborundum Corporation have been in test 52 days. The behavior is similar to that of comparable alloys made here.

Eleven samples of Zr-Ni-Fe and Zr-Cu-Fe alloys have been tested for 260 days. All samples have developed relatively thick films. Prior to 220 days the Zr-Cu-Fe samples displayed generally smooth films with edge splitting. The effect of prior cold rolling was small. Quenching from 900°C prior to test appeared to be deleterious. The Zr-Ni-Fe sample formed generally uniform films with edge splitting. Weight gains were higher than in Zr-Cu-Fe, the eventual rate of gain being, however, only slightly higher. Both cold rolling and quenching seemed to be deleterious.

Powder products of Zr-Ni-Fe and Zr-Cu-Fe made by compacting mixtures of the elemental powders displayed moderate corrosion resistance during a 52-day test. A sample of compact made from powdered Zr-Cu-Fe alloy was severely attacked during a 20-day exposure.

Edge splitting of the corrosion film has now occurred in all Zr alloy and powder compact samples exposed to this environment. A few samples exhibit surface blemishes which are not yet understood.

(2) Tests in Oxygenated Steam at 650°C, 600 psi - After 33.5 days in steam containing about 30 ppm oxygen, Zr-1 w/o Cu-1 w/o Fe was superior to Zr-3 w/o Ni-0.5 w/o Fe. The best sample gained weight at about 10 mdd (linearly) after a week, but developed edge cracks in the film in less than one week. The corrosion behavior is similar to that in deoxygenated conditions.

(3) Tests in Deoxygenated Water at 360°C - Since superheat fuel elements and other structural members will be periodically exposed to high temperature water, it is necessary to know the behavior of alloys of interest under these conditions. Preliminary results are as follows. During nearly 2 months' exposure, as-cast samples of Zr-Ni-Fe and Zr-Cu-Fe alloys showed good corrosion resistance, the latter gaining weight at a somewhat lower rate. Of hot rolled samples only the Zr-Ni-Fe sample from batch AE 10 was resistant; another sample from batch

AE 39 was not. Neither Zr-Cu-Fe sample was good. A sample compacted from powdered Zr-Cu-Fe alloy was destructively attacked during a short exposure.

b. Lightweight Alloy for Use with Mercury - A loop test was made to study the effects of mercury velocity on corrosion and possible mass transfer of nitrided commercially pure titanium. The loop is constructed of quartz and flow is produced by a temperature differential (thermal convection). An average flow rate of 8.2 ft per minute and a temperature differential of 96°C (371-275°C) was maintained. After 720 hours of temperature differential operation, mass transfer was not detected. Metallographic examination indicated that there is an even nitrided layer over large recrystallized grains. The inner structure consists of relatively large equiaxed alpha grains with heavy precipitates in both the grains and grain boundaries. There was no evidence of attack on samples in either the hot or cold legs.

2. Irradiation Studies

a. Preirradiation Testing of Cobalt-Dysprosium Oxide Absorber Specimens - Rare earth oxide dispersions are being studied at Argonne for their utility as possible improved control rod materials. As a part of this study, the structure, hardness, compressive strength, thermal stability, and corrosion resistance of pressed and sintered pellets of cobalt and Co-30 w/o Dy_2O_3 were determined. X-ray diffraction analyses and metallography indicated that the cobalt in both compositions was fine grained alpha cobalt (hexagonal). The cobalt and Co-Dy_2O_3 samples had R_A hardness values of 55 to 56 and 42 to 46 respectively. A standard Rockwell hardness tester was used for all the hardness tests.

(1) Compression Tests - Four pellets, two containing cobalt of 99.8% purity and two containing Co-30 w/o Dy_2O_3 were used for compression testing. A tensile machine was used for these tests, utilizing two machined blocks of low-carbon steel as contact surfaces and a feed rate of 0.002 in. per minute. The small size of the samples, as well as the nature of the test itself, did not allow the determination of the yield strength of the materials. Values for the ultimate compressive strength and corresponding changes in physical dimensions are given in Table IX. The samples ruptured in a diagonal direction along the length of the samples.

(2) Thermal Tests - The furnace used for the thermal cycling and thermal shock tests provided a helium atmosphere around the specimens during both types of test. Before the tests were conducted, a temperature profile was determined for the furnace. The samples and recording thermocouple were placed at the point of maximum temperature during all tests.

Table IX. Compression Test Data on Pressed and Sintered Pellets of Cobalt and Co-30 w/o Dy_2O_3

Sample	Initial Sample Diameter, in.	Initial Sample Length, in.	Ultimate Compressive Strength, psi	Max. % Increase In Cross-Sectional Area	% Total Length Decrease
Cobalt	0.200	0.338	211,000	48.5	27.5
Cobalt	0.200	0.367	210,000	44.0	27.0
Co-30 w/o Dy_2O_3	0.200	0.468	112,000	37.0	19.4
Co-30 w/o Dy_2O_3	0.200	0.465	107,000	-	-

One pellet containing Co-30 w/o Dy_2O_3 was cycled between 300°C and 700°C. The pellet was placed in the furnace, brought to temperature, and held for 20 to 25 minutes after which the furnace power was shut off and the sample was allowed to cool to between 280°C and 300°C. This allowed the sample to pass through the alpha to beta transformation temperature of 420°C to 480°C during each cycle. The pellet was cycled for 125 times. Macro examinations and dimensional checks were made at periodic intervals throughout the test.

The dimensional changes were slight, being less than 1 percent in any given direction, and this change was partially, if not wholly, due to Co_3O_4 which formed on the surface of the pellet. X-ray diffraction studies made at the end of the test indicated an alpha cobalt matrix and cubic Dy_2O_3. The metallographic examination indicated that very little grain growth had occurred, possibly because of the restraint afforded by the Dy_2O_3 particles. No reaction zone was found in any of the samples examined in the as-polished condition.

Two pellets, one containing cobalt of 99.8% purity and the other containing similar cobalt with the addition of 30 w/o Dy_2O_3, were subjected to thermal shock tests. The tests consisted of repeated quenching from temperatures between 400°C and 1000°C down to room temperature. Initially, the pellets were placed in the furnace, brought to a temperature of 400°C, and held at that temperature for ten minutes to insure a uniform pellet temperature, then quenched in cold running water. This cycle was repeated five times after which the samples were removed from the furnace so that a visual examination and dimensional measurements could be made. This process was repeated at 100°C intervals until a temperature of 1000°C was reached.

Cracks first began to appear in the Co-Dy_2O_3 pellet after quenching from 800°C and became more pronounced as the temperature was increased. However, at no time during the test did the pellet shatter or fracture. A possible explanation for the observed cracking lies in the

difference between the thermal expansion coefficients of the oxide and the cobalt matrix. A metallographic examination of both specimens was made at the conclusion of the tests. The cobalt sample showed extensive grain growth and some grain coarsening in areas near the pellet surface. Grain growth was not evident in the Co-Dy_2O_3 specimen. X-ray diffraction analyses indicated that the cobalt in both samples was alpha and that the Dy_2O_3 had remained cubic.

(3) Corrosion Tests - Two pellets containing Co-30 w/o Dy_2O_3 were corrosion tested in boiling distilled water. Sample 1 was in the as-sintered condition and had been intentionally scored and struck several times to simulate the results of extremely rough handling. Sample 2 was centerless ground to a diameter of 0.208 in. The pellets were immersed in boiling distilled water for a total of 1012 hours and showed weight gains of 0.30 and 0.47 percent.

The only noticeable corrosion was a slight attack on some of the Dy_2O_3 located at the surface of Sample 2. The results are encouraging since the Dy_2O_3 used in the pellets was not stabilized and should not be particularly corrosion resistant. Some of the pellets are being tested in high temperature steam where corrosive attack should be accelerated.

3. Metallic Fuel Studies

a. Thorium-Uranium-Plutonium Alloys - Three thorium-uranium-plutonium alloys have been selected for the initial series of property determinations and irradiation testing with a view toward evaluating their potential as fast reactor fuels. Their compositions in weight percent are:

1. 60 Th-20 U-20 Pu
2. 75 Th- 5 U-20 Pu
3. 80 Th-10 U-10 Pu

Alloy 1 was chosen as being representative of a fuel suitable for an EBR-II size reactor; Alloy 2 is a fuel composition which is potentially suitable for intermediate size power reactors; Alloy 3 may satisfy the fuel requirements of a very large power reactor.

The alloys were prepared from commercial Th-(93% enr.)U and reactor plutonium. Alloy 1, 60-20-20, which has a liquidus temperature around 1250°C, was then injection cast in a new experimental injection casting unit. Two good pins were obtained of 12 in. length, nominal 0.144 in. diameter and uniform density as observed by cobalt-60 radiographs.

The much higher melting Alloy 2, 75-5-20, could not be injection cast into Vycor molds. The molds softened at the higher temperature. Mold materials other than Vycor are presently being investigated.

4. Nondestructive Testing

a. Inspection of Niobium Tubing - An attempt has been made to evaluate one $\frac{3}{4}$ in. diameter niobium tubing. Because none of the niobium tubing could be spared for preparation of a standard, a substitute metal was needed. A search of available literature revealed that the ultrasonic shear-wave velocity in niobium is almost matched by that in both copper or brass. Therefore, a 6 in. piece of copper was fabricated for use as the standard. This copper standard contains two V-notches, one on the I.D. and the other on the O.D. Both notches are four mils deep and $\frac{1}{2}$ in. long. The O.D. notch runs circumferentially while the I.D. notch is oriented along the longitudinal axis of the tube. Utilization of such a standard makes it impossible to judge the depth of a defect although one can be certain of the system's ability to detect I.D. flaws.

b. Neutron Imaging - The neutron radiographic facility at the JUGGERNAUT reactor has been used to perform inspections on three radioactive, irradiated reactor fuel capsules. Previous inspections of these capsules had been completed using an autoradiographic, pinhole camera method (described in ANL-6533), but further improvements in image quality were desired.

Neutron radiographic inspection is useful in this case because the use of transfer exposure methods eliminates the interference which the radioactive decay radiation from the capsules would produce on the X-ray film in a normal radiographic inspection. In a neutron transfer exposure method, the only problem introduced by the radioactive nature of the inspection objects is the personnel hazard. A heavy-density concrete block wall was employed in these preliminary tests to reduce that problem.

A transfer exposure technique employing a combination of a dysprosium metal screen backed by a silver screen was used for most of the exposures. After the neutron exposure, the screens were transferred to different cassettes. The silver was transferred to a fast film which could be developed within a few minutes to yield an immediately available picture to determine the alignment of the inspection object.

The dysprosium was transferred to a cassette loaded with a finer grain film and required a several hour decay time before the film could be processed. The use of this double transfer screen technique was valuable because it was not necessary to wait several hours for the finer grain film image to determine whether the inspection object was oriented correctly in the neutron imaging beam. This double screen transfer exposure technique will also prove useful in other applications.

The contrast and detail on the neutron radiographs of the fuel specimens have been very good. A lead container is now being considered

to provide improved radiation shielding and to simplify some exposure details. With the availability of this container, neutron radiographic inspection of radioactive reactor fuel capsules is expected to become routine practice.

c. Mass Absorption Coefficient Method for Measuring Uranium Content - A method of measuring uranium content of samples by measuring the mass absorption coefficient for a monochromatic X-ray beam is being studied. The reduction of intensity of an X-ray beam passing through an absorber is given by

$$I = I_0 e^{-\mu_m \rho t}$$

where μ_m is the mass absorption coefficient, ρ is the density and t is the thickness. For a two component system the expression can be written as

$$\ln \left(\frac{I_0}{I}\right) = \mu_1 \rho t w_1 + \mu_2 \rho t w_2$$

where w_1 is the weight fraction of the component having mass absorption coefficient μ_1 and w_2 is the weight fraction of the component having mass absorption coefficient μ_2.

Since $w_2 = 1 - w_1$ the formula can be reduced to

$$\frac{\ln \left(\frac{I_0}{I}\right)}{\rho t} = (\mu_1 - \mu_2) w_1 + \mu_2$$

The product ρt can be replaced by the ratio $w/A = \rho t$ where w is the total weight of the sample and A is the area. The mass absorption coefficient for the two components can be measured. The weight and area of the sample are also measurable quantities. Therefore the above equation can be solved for w_1 which, when multiplied by 100, gives the weight percent of component 1 in the sample.

To determine the feasibility of the technique the mass absorption coefficients of 2 in. sq. clad samples from BORAX-V superheater plates were determined for an energy of 58 kev. The results are given below:

Sample No.	w/o U (estimated)	w/o U (calculated from mass absorption coefficient)
HCE 87	4.41	4.15
HPE 227	6.61	6.86
FCE 55	8.12	8.02
FPE 255	12.52	12.64

d. Tests on Refractory Alloy Tubing - This tubing is intended for use in irradiation and other type tests and is being tested nondestructively by pulsed-field equipment which is itself under development. Three different objects are being accomplished by these tests:

(1) The quality of the tubing itself is revealed, knowledge of which can eliminate a previously unknown factor in some of the irradiation experiments.

(2) Test experience is acquired on a considerable variety of materials, of which at least some will appear in future reactor cores.

(3) The performance of the test equipment itself can be carefully studied under a wide variety of operating conditions. This is the best way to determine what improvements are needed in future test systems.

As a part of this effort, 400 ft of niobium-1 w/o zirconium tubing of 0.156 in. I.D. x 0.010 in. wall was tested by developmental pulsed-field equipment in lengths of about 4 ft. About half of these tubes contained localized defects extending between 10 and 60 percent of the wall thickness. Since the tubing was to be used in lengths of less than 4 in., the defective areas were marked and cut out. These amounted to about 50 separate defects totaling about 16 ft.

C. Reactor Components Development

1. Development of Manipulators for Handling Radioactive Materials

a. Model A Manipulator Seal Test - A motion seal of the type used in the sealed mechanical master-slave manipulator (CRL Model A) supplied by Central Research Laboratories has been tested under simultaneous conditions of a dry atmosphere and intense irradiation. The seal was a $\frac{3}{8}$ in. seal, No. 1035, supplied by Chicago Rawhide. The seal was turned at 100 rpm during the period of leak testing and the torque was measured by the use of two autosyns mounted so that the deflection of a shaft driving the seal was determined.

The seal was maintained in a dry nitrogen atmosphere which varied from 12 to 30 ppm. During the course of the test the seal received a gamma exposure of 3×10^9r from mixed fission products and it was turned 35,000 revolutions. The torque remained 4 and 6 in./oz during the test, with the average torque decreasing slightly. The nitrogen leakage, with a differential pressure of 3 inches across the seal, has remained near 0.1 cu in./day. Although the sensitivity of the leakage test is close to the observed leak rate there was some indication of a small increase in leakage as the test proceeded. The results seem to indicate that the seal could be used for higher exposures than 3×10^9r and for more than 35,000 revolutions with a dry nitrogen atmosphere.

2. Development of Viewing Systems

a. Electrical Properties of Glass - Studies on the electrical properties of glass have been continued along two general lines, namely, to achieve a better understanding of the radiation induced coloration of glass, and the phenomenon of radiation induced voltage build-up which has resulted in the dielectric break-down and fracture of glass in a few shielding windows. The over-all objective is to achieve a practical shielding glass with improved resistance to radiation induced coloration and breakage.

Most of the experimental investigation has centered on observing the charge displacement that occurs when an irradiated glass sample is heated between electrodes in the absence of externally applied voltage, but with a thermal gradient across the glass sample. These so-called thermo-electric measurements were originally performed with temperature gradients of 20 to 40°C/mm. A new apparatus has been developed which allows measurements at a considerably lower gradient of about 2°C/mm. It was thought that at this lower gradient a more sensitive test could be made for localized space charges that could contribute to dielectric break-down.

It has been found that this test is very sensitive to heterogeneities in the glass sample. Reproducible results have been obtained using a borosilicate glass by bubbling oxygen through the glass melt to produce thorough homogenization. A useful feature of the new apparatus is that the temperature gradient can be reversed without disturbing the sample. By this means it has been observed that the charge displacement reverses completely with the gradient. This observation supports the previous interpretation that the charge displacements occur as a result of the thermal gradient.

D. Reactor Materials Development

1. Radiation Damage to Reactor Structural Materials

a. Irradiations of Steel in EBR-I - Preliminary impact test data from typical SA-212B carbon steel irradiated in EBR-I are shown in Figure 2 and summarized in Figure 3. The abscissa in Figure 3 is a measure of exposure based on the energy-dependent model, and does not imply that such a number of defects actually survive after initial collisions. These points are obtained from data which suffer from sufficient scatter so that one cannot confidently assign a slope value to the curve. Some duplicate irradiations have been completed and the specimens will be tested.

The samples for the last irradiations to be performed in EBR-I are being prepared. The material will consist of single crystals

of copper and silver contained in leak-tight steel capsules filled with sodium as a thermal bond. The EBR-I is scheduled for reloading with the Mark-IV core and further irradiation testing is not now contemplated.

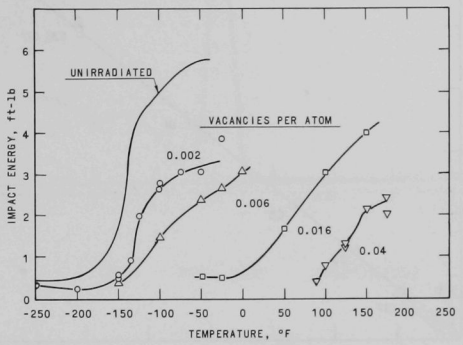

Figure 2. Impact Properties of SA-212B; EBR-I Irradiations

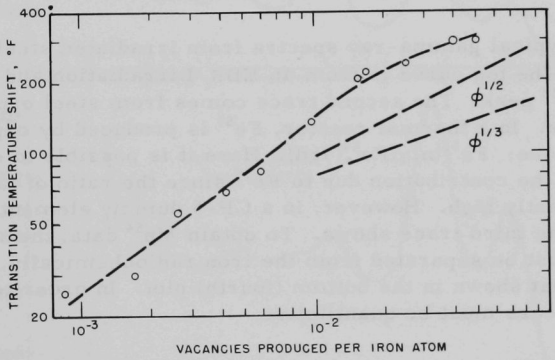

Figure 3. Transition Temperature Shift As a Function of Exposure: EBR-I

b. Dosimetry - Chips were taken from each steel specimen irradiated in EBR-I and the Mn^{54} activity was counted. This nuclide, with its 314-day half-life, appears to be a very promising monitor for long-term neutron damage studies. The correlation between exposure time and observed activity, with corrections made for decay, is shown in Figure 4.

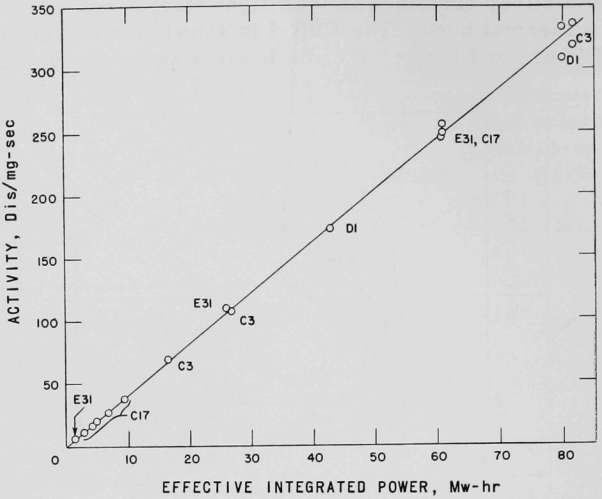

Figure 4. Correlation of Mn^{54} Activity with Predictions

Typical gamma-ray spectra from irradiated steel are shown in Figure 5. The top curve is from an EBR-I irradiation and clearly shows the Mn^{54} peak. The second trace comes from steel exposed in a CP-5 fuel tube. In a thermal reactor, Fe^{59} is produced by capture of thermal neutrons: $Fe^{58}(n,\gamma)Fe^{59}(46d)$. Here it is possible to correct the Mn^{54} peak for the contribution due to Fe^{59} since the ratio of fast-to-thermal flux is sufficiently high. However, in a CP-5 dummy element, this is not the case, as the third trace shows. To obtain Mn^{54} data, the radioactive manganese must be separated from the iron radiochemically, and yields a trace like that shown in the bottom (fourth) plot. In order to be of value this process must be quantitative.

Preliminary tests on the efficiency of the radiochemistry on EBR-I material produce yields in the range of 80% to 90%. Current work is directed toward improving the procedure to make it more quantitative.

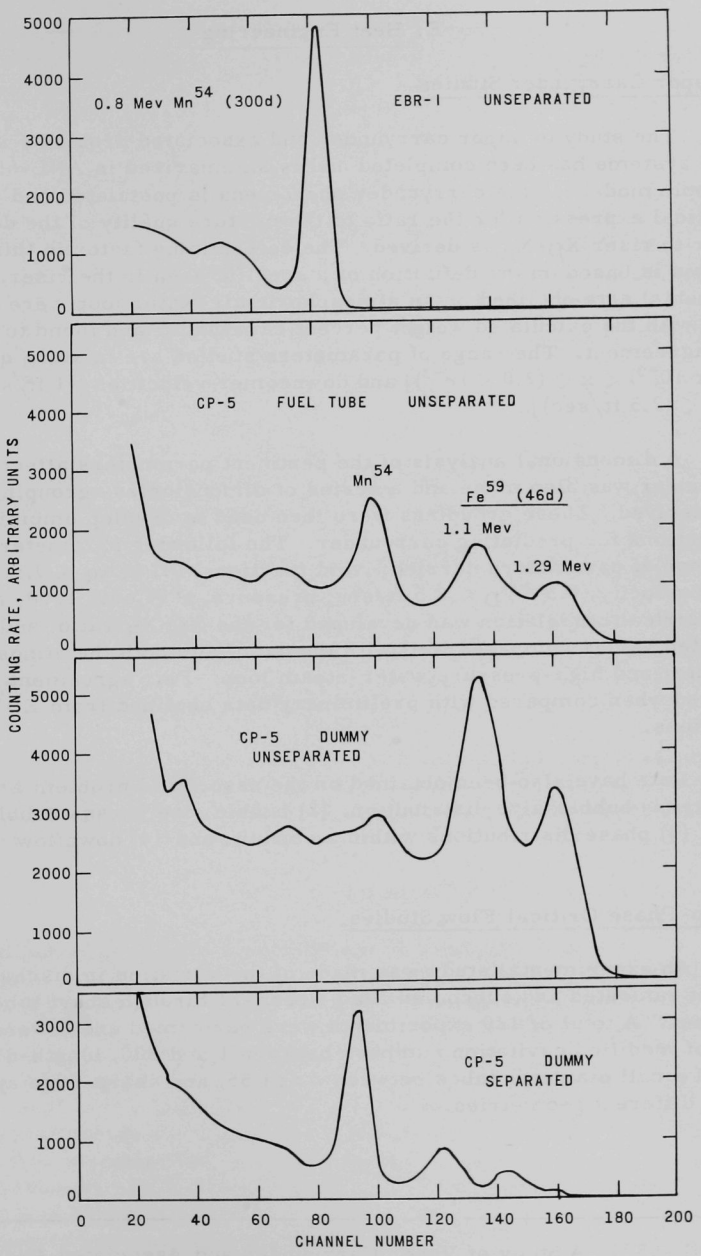

Figure 5. Typical Gamma-Ray Spectra from Irradiated Steel

E. Heat Engineering

1. Vapor Carryunder Studies

The study of vapor carryunder and associated problems in two-phase systems has been completed and is summarized in ANL-6581.[1] A simple model for the carryunder phenomena is postulated and an analytical expression for the ratio of the mixture quality of the downcomer to riser X_D/X_R is derived. The determining factor in this analysis is based on the definition of a specific area in the riser. Experimental data obtained on an atmospheric air-water loop were compared with the calculated weight percent carryunder and found to be in good agreement. The range of parameters studied are mixture qualities $[(0.2 \times 10^{-3}) < x < (2.0 \times 10^{-3})]$ and downcomer velocities [(1 ft/sec) $< V_D <$ (2.5 ft/sec)].

A dimensional analysis of the pertinent parameters affecting carryunder was also made and a series of dimensionless groupings were derived. These groupings were then used to develop empirical correlations for predicting carryunder. The following parameters cover the range of parameters carried: void fractions, $0.1 < \alpha_R < 0.5$; downcomer velocity, $0.5 < V_D < 2.5$ ft/sec; pressure, P = 600, 1000, 1500 psi. An empirical correlation was developed for the X_D/X_R ratio, and its predicted values compared well with the data from both the atmospheric air-water and high-pressure water-steam loop. Fair agreement was also achieved when compared with preliminary data obtained from EBWR operations.

Data have also been obtained on the associated problem areas, namely: (1) bubble-size distribution; (2) bubble size versus bubble velocity; (3) phase distributions within a conduit; and (4) downflow slip ratios.

2. Two-Phase Critical Flow Studies

An experimental study was made of the variation in discharge rates of saturated and subcooled fluid Freon-11 through short tubes and apertures. A total of 120 experiments were performed and covered a range of modified cavitation numbers between 1 and 500, length-diameter ratio of small diameter tubes between 2 and 55, and sharp-edge apertures of nine different geometries.

---

[1] ANL-6581, A Study of Vapor Carryunder and Associated Problems, Michael Petrick.

It was found that below the modified cavitation number of 10 the fluid exhibits completely metastable single-phase flow. In the range of modified cavitation numbers between 10 and 14, unstable transitional flow occurs. When the modified cavitation number exceeded 14, two-phase critical flow seemed likely to occur.

The Euler number may be correlated with the modified cavitation number and length-diameter ratio. Discharge rates can thus be determined from the correlations. Euler numbers for the apertures of various configurations including square, rectangular, and eye-shaped were found to be in the same order of magnitude as those of circular shapes. Triangular and W-shaped orifices were found to possess lower Euler numbers than the circular ones.

3. Boiling Liquid Metal Studies

An investigation of possible laboratory techniques to supply a heat flux in excess of 10^6 Btu/(hr)(ft^2) to flowing alkali metal was conducted. Electron beam heating techniques show promise for this application. Basically the system consists of two concentric tubes, with heat applied to the inside surface of the inner tube while the liquid metal is passed in the annulus between the tubes. The heating is accomplished by placing an electron emitter (cathode) inside of the evacuated inner tube and directing the electrons to impinge upon the inside surface of this inner tube which serves as the anode. The heat generated then flows through the tube wall to the flowing liquid metal in the annulus.

A small electron beam heating model was constructed and established the feasibility of the concept. A working model is being constructed to be used in developing the technology and for possible use in experimental work.

F. Chemical Separations

1. Fluidization and Volatility Separations Processes

a. Fluoride Separations - A proposed method for separating plutonium hexafluoride from uranium hexafluoride depends upon the selective thermal decomposition of plutonium hexafluoride at 250° to 300°C. Experiments which have been reported previously (see Progress Report for July 1962, ANL-6597, page 41) were undertaken to determine whether uranium hexafluoride undergoes decomposition at about 300°C. In the course of this investigation, it was found that a residual gas, which was noncondensable at -196°C, was formed when uranium hexafluoride was heated for five hours at 330°C in a welded nickel vessel in which the reaction products were allowed to accumulate. When the reaction vessel was opened, it was observed that the solid reaction product, uranium

tetrafluoride, was located only near the weld areas, which strongly suggested a corrosion type reaction. Mass spectrographic analysis showed the gas to contain 94.1 percent oxygen, 3.6 percent nitrogen, and 2.3 percent water. Fluorine was not found in the gas mixture. The sources of nitrogen and water are not known with certainty, but are believed to be a small air leak and the outgassing of the vacuum line associated with the mass spectrograph. The most likely source of oxygen is considered to be nickel oxide which was probably formed during the welding of the nickel vessels. The formation of oxygen from the nickel oxide is attributed to the following reaction:

$$UF_6 + NiO \rightarrow NiF_2 + UF_4 + \tfrac{1}{2} O_2$$

In this reaction, the ratio of moles of gas produced to moles of uranium hexafluoride consumed is 0.5. This is in fairly good agreement with the ratios reported previously, which ranged from 0.35 to 0.61 for five-hour reaction periods at 330°C. On the basis of these findings, it has been concluded that uranium hexafluoride did not undergo thermal decomposition at 330°C.

The effect of gamma radiation on plutonium hexafluoride is being investigated as part of a fundamental study of the radiation behavior of plutonium hexafluoride. Current experiments are designed to obtain information concerning the mechanism of the gamma ray induced decomposition of plutonium hexafluoride. The variation of decomposition with dose, and the effect of the presence of the diluent gases helium, krypton, and oxygen on the decomposition of plutonium hexafluoride under gamma radiation has been previously reported (see Progress Report, June 1962, ANL-6580, page 42). Experiments on the irradiation of plutonium hexafluoride samples containing helium at one and two atmospheres helium pressure with gamma doses of 10^8, 2×10^8, and 3×10^8 rad confirm the previously reported negligible effect of helium on the gamma radiation decomposition of plutonium hexafluoride. Similar experiments with krypton resulted in a much smaller G value at two atmospheres krypton pressure than at one atmosphere (4 vs 14). This apparent pressure effect will be investigated further. The presence of oxygen appears to inhibit decomposition of plutonium hexafluoride by gamma radiation. The products of decomposition will be identified in order to determine if a chemical reaction is taking place between plutonium hexafluoride and oxygen.

b. Direct Fluorination of Uranium Dioxide Fuel - Laboratory work in the direct fluorination process has been directed toward investigating a process modification which involves the oxidation of the uranium dioxide pellets to U_3O_8 powder prior to the fluorination step (see Progress Report, August 1962, ANL-6610, page 55). When the uranium oxide is in the form of a uniform, fine powder, complete fluorination of the plutonium to the hexafluoride is easier to carry out. In previous experiments, about

99.4 percent of the plutonium was removed from mixtures of uranium dioxide, plutonium dioxide and selected fission product element oxides, after oxidizing the mixtures and subsequent fluorination.

Current fluorination experiments were conducted to determine the minimum fluorination time and temperature needed to remove 99 percent of the plutonium from the product of the oxidation step. This oxidation product is a mixture of the oxides of uranium (U_3O_8) and plutonium (PuO_2) containing about 0.3 wt-% plutonium and about one wt-% of a mixture of 10 fission product element oxides (BaO, ZrO_2, La_2O_3, CeO_2, Y_2O_3, Nd_2O_3, Sm_2O_3, Pr_6O_{11}, Eu_2O_3, and Gd_2O_3). It is mixed with Alundum prior to reaction with fluorine. In a series of five experiments performed at 450°C utilizing a mixture of 10 percent fluorine, 25 percent oxygen and 65 percent nitrogen, the fluorination times were from two to eight hours. After a reaction time of two hours, essentially all of the uranium and about 90 percent of the plutonium were removed from the solid mixture; an increase of the reaction time to eight hours produced no additional removal of plutonium. In the present study a second fluorination using 75 percent fluorine and 25 percent oxygen at 550°C for five hours was necessary to achieve 99 percent removal of the plutonium.

The kinetics of the reaction between U_3O_8 and fluorine are of interest to the direct fluorination process in view of the ease of removal of plutonium from oxidized solid solutions of PuO_2 in UO_2. Preliminary results have been obtained for the kinetics of the fluorination reactions of U_3O_8, UO_2F_2, and UO_3 using a thermobalance. Data were obtained for the fluorination of UO_2F_2 and UO_3 because these compounds may be intermediates in the fluorination of U_3O_8. The kinetic treatment used for the data obtained for these fluorinations is based on a diminishing sphere model. In this model, the reaction rate is related to the fraction of the solid unreacted by the expression $(1-F)^{1/3} = 1 - k't$. The rate term k' can be obtained from the slope of a plot of the function $(1-F)^{1/3}$ versus t where F is the fraction of solid reacted in time t. Values of $k' \times 10^3$ in min^{-1} obtained in this preliminary work varied from 0.2 to 380 for the temperature range 240° to 300°C for U_3O_8, from 0.3 to 22 for the range 200° to 340°C for UO_2F_2, and from 1 to 8 for the range 290° to 340°C for UO_3. Activation energies of 75, 17, and 27 kilocalories per mole were calculated for the fluorination reactions of U_3O_8, UO_2F_2, and UO_3, respectively.

Engineering-scale studies have continued on developing a two-zone oxidation-fluorination scheme (see Progress Report, August 1962, ANL-6610, page 55) for the production of uranium hexafluoride from uranium dioxide pellets, the reactions being carried out in a single reactor. In this proposed process uranosic oxide (U_3O_8) fines are formed by oxidation of uranium dioxide pellets in a lower zone static pellet bed, elutriated by a mixture of oxygen and nitrogen, and fluorinated with fluorine in an upper zone fluidized bed of Alundum. The oxygen-nitrogen mixture is

introduced at the bottom of the reactor and the fluorine gas is introduced at the top of the uranium dioxide pellet bed. It is desirable to equalize the rates of (1) fines formation, (2) removal by elutriation from the pellet bed, and (3) fluorination in the fluidized bed of Alundum. Equalization of these rates will avoid fines buildup in the uranium dioxide pellet bed and/or slugging of large quantities of fines to the fluorination zone. This will improve fluorine efficiency and minimize elutriation of fines from the upper zone. Three methods of achieving equalization have been investigated: (1) The use of gas back-diffusion to provide selective oxidation of the uranium dioxide pellets at the top of the pellet bed rather than throughout the depth of the bed. This method would allow use of much higher oxygen concentrations, e.g., the use of air which is 21 percent oxygen rather than the 8 to 11 percent oxygen which is presently considered the maximum safe operating level with a pellet bed temperature of 400° to 500°C. However, a test of this method produced no U_3O_8 fines and therefore this approach does not appear to be feasible. (2) The maintenance of a temperature gradient from top to bottom of the pellet bed so that the top is at 400° to 500°C and the bottom at a much lower and therefore unreactive temperature. This method would also allow use of much higher oxygen concentrations because the majority of the reaction would occur at the top of the pellet bed thus minimizing operational problems such as caking. Preliminary data from a run using this method indicate that the rates of fines formation and elutriation are closely matched. High oxygen concentrations (17 and 30 percent) have been passed through the pellet bed successfully, with freedom from caking, and steady production of uranium hexafluoride at a rate of 40 lb/(hr)(sq ft reactor cross section). (3) The pulsing of the gas going through the bottom of the column to control the elutriation of fines from the pellet bed in the lower zone. Preliminary results of tests in a 3-inch diameter lucite-glass column containing a 6-inch bed of pellets have shown that a momentary 12 percent increase in pellet bed void volume can be achieved with a pulse lasting less than 0.1 second from a 20 psig supply. This pulse was sufficient to move the entire bed of pellets one inch up the column. The pulse also re-orients the pellets so that gas paths through the bed are changed after each pulse, thus minimizing fines holdup and helping to reduce channeling of gas through the bed.

Measurement of effective thermal conductivities (k) in the axial (longitudinal) direction of 4-in. diameter fluidized-packed beds was carried out at 50°C bed temperature and superficial gas velocities from 0.0 to 1.0 ft/sec for several packing shapes and fluidizing media. Typical results for those fluidized-packed runs for 0.5 ft/sec gas velocity are given in Table X. The data show that a reduction in fluidizing particle size increases the heat transfer. Longitudinal heat-transfer coefficients in a fluidized-packed bed increase with superficial air velocity to a maximum value between 0.4 and 0.7 ft/sec. Above that velocity the thermal conductivity remains constant or drops. These tests also indicated that

longitudinal heat transfer is greater than radial heat transfer by a factor of approximately 10. For the case of open-tube fluidization the heat transfer was so rapid that there was no distinguishable difference in the longitudinal temperatures. From these results it would appear more efficient to remove heat from a fluidized zone at the top or bottom of a large diameter reactor rather than radially through the walls of the packed section.

Table X. Effective Thermal Conductivities

Arrangement of Packed-Fluidized Bed		Results
Packing	Fluidizing Medium	Values of k at 0.5 ft/sec superficial gas velocity (Btu/(hr)(sq ft)(F/ft))
$\frac{3}{8}$- x $\frac{3}{8}$-in. brass cylinders	70 mesh glass beads	91
$\frac{3}{8}$- x $\frac{3}{8}$-in. brass cylinders	120 mesh glass beads	300
$\frac{3}{8}$- x $\frac{3}{8}$-in. brass cylinders	-56 + 100 mesh Alundum	109
$\frac{1}{2}$-in. steel spheres	-56 + 100 mesh Alundum	601

c. Separation of Uranium from Zirconium Alloy Fuels

(1) Studies of the Chlorination and Fluorination Steps with Down-Flow Fixed-Bed Filters - Studies continued on the development of a fluid-bed volatility process for the recovery of uranium from highly enriched uranium-zirconium alloy fuels (see Progress Report, July 1962, ANL-6597, page 43). A chlorination-fluorination reaction sequence currently being evaluated includes hydrochlorination followed by reaction with phosgene, hydrofluorination and a final fluorination step. A 12-hour run was made using this sequence. This run included 5 hr of reaction with hydrogen chloride at 400°C fluid-bed temperature, 1 hr of reaction with phosgene at 400°C, 2 hr of reaction with hydrogen fluoride at 400°C, a 2-hr fluorination with fluorine at 400°C, followed by a second fluorination with fluorine for two hours at 500°C. During the phosgene and hydrofluorination steps the down-flow filter bed of Alundum was maintained at 370°C. For the remaining periods it was maintained at the fluid-bed temperatures. Of the initial charge (240 g of 5.1 wt-% uranium-Zircaloy alloy chips) 0.7 percent was retained by the Alundum (Type RR) in the fluidized bed and 0.3 percent by the Alundum (Type RR and Type 38 in weight ratios 9:7, respectively) in the filter bed. Other uranium losses included 0.4 percent through the filter to the zirconium tetrachloride condenser during chlorination and 0.3 percent to the alumina fluorine disposal column

downstream of the uranium hexafluoride collection cold traps during fluorination. A material balance showed the remaining uranium was either collected in the cold traps as hexafluoride (93.6 percent collection) or associated with samples of bed material taken during the run (5.6 percent). Results of analyses of samples taken at half-hour intervals throughout the run indicated it may be feasible to reduce the cycle time to about nine hours from the 12-hour cycle time actually used in this experiment by reducing the hydrofluorination, fluorination and refluorination times from 2 hr each to 1 hr each.

(2) Fluid-Bed Hydrolysis of Zirconium Tetrachloride - The hydrolysis of zirconium tetrachloride to zirconium dioxide by steam in a fluidized bed of Alundum was studied further. The effects of the operating conditions of bed height, temperature and starting bed particle size on the deposition (conversion) of the dioxide on the bed material were evaluated. Results evaluated on the basis of the quantity of fines (-200 mesh material) produced in a given run showed: (a) no effect of bed height, (b) a possible effect of temperature, a medium temperature of 350°C being better than 250°C or 500°C and (c) no marked effect of starting bed particle size.

2. Chemical Metallurgical Process Studies

a. Chemistry of Liquid Metals - The solubilities of technetium in liquid zinc were found to range from 2.0×10^{-3} wt-% at 470°C to 0.12 wt-% at 758°C.

An experiment to investigate the possibility of intermediate phases existing in the tungsten-zinc system has been performed. Zinc-tungsten compacts containing 12 to 81 percent zinc, which had been heated for about two weeks at 430°C and for $4\frac{1}{2}$ weeks at 650°C, were examined by metallography and X-ray diffraction. There was no evidence that an intermediate phase exists.

Data reported earlier (see Progress Report for January 1962, ANL-6509, page 43) for the solubility of beryllium in liquid zinc at 429° to 611°C have been extended to higher temperatures. The solubilities have been found to range from about 0.1 wt-% (a maximum) at 690°C to about 0.03 wt-% at 830°C.

An experiment was performed to determine whether amounts of iron up to about 0.2 wt-% in zinc solutions appreciably affect the solubility of uranium. Preliminary analysis of data obtained at 655°C reveals that there is no significant loss of uranium from solution.

In further study of the uranium-zinc binary system, the melting point of the delta phase, $UZn_{8.5}$ was determined by means of thermal analysis. The melting point was found to be 938° ± 2°C, which may be compared with the literature value of 944° ± 5°C.

Emf data for the galvanic cell, $Pu/PuCl_3$, LiCl-KCl/Pu-Zn (two-phase alloy) have been obtained in a new cell over the temperature range, 485° to 619°C. The new cell was similar to the preceding one except that an alumina thermocouple tube was used in place of a quartz tube. The emf values, which were lower than those obtained in the preceding cell (see Progress Report for August 1962, ANL-6610, page 58), may be represented by the equation

$$E \text{ (volts)} = 1.142 - 7.5_9 \times 10^{-4} T \quad .$$

The calcium-zinc phase diagram has been re-examined by differential thermal analysis, X-ray diffraction analysis, and vapor effusion measurements. The results indicate that the compounds, $CaZn_2$, $CaZn_5$, and $CaZn_{11}$, melt congruently at 704°, 695°, and 724°C, respectively; the compounds, Ca_3Zn, Ca_7Zn_4, CaZn, Ca_7Zn_{20}, and $CaZn_{13}$, melt incongruently at 394°, 414°, 439°, 642°, and 669°C, respectively.

b. Calorimetry - The final value for the heat of formation of aluminum fluoride is -356.5 ± 0.7 kcal/mole. This may be compared with the preliminary value of -359 kcal/mole (Progress Report for July 1962, ANL-6597, page 45) and with recent literature values of -356.3 kcal/mole, -357.0 ± 2 kcal/mole, and -358.2 ± 1.4 kcal/mole.

A final series of combustions of uranium in fluorine has been completed. Calculation of the enthalpy of formation of uranium hexafluoride gas is proceeding.

IV. PLUTONIUM RECYCLE

The EBWR Core 2 design will be used in the plutonium recycle study. The core will consist of the central (6 x 6 = 36 fuel subassemblies) zone loaded with PuO_2-UO_2 fuel and the remainder of the core will be fueled with slightly enriched UO_2. Various central zone enrichments will be examined and particular attention will be given to the control characteristics of the various configurations.

An extensive series of GAM-I, MUFT-4, and Sofocate calculations have been made to establish the seven-group cross sections required for studying the two-zone loading for the EBWR. The GAM-I results will be used for the fast cross sections with the exception of the Pu^{240} resonance cross section which will be obtained from MUFT-4. Resonance self-shielding factors for the uranium and plutonium isotopes are also being obtained from MUFT calculations. The thermal cross sections are being obtained from the Sofocate code.

V. ADVANCED SYSTEMS RESEARCH AND DEVELOPMENT

A. Argonne Advanced Research Reactor (AARR)

1. Core Physics Calculations

The sensitivity of core reactivity to possible variations in the metal cross sections was checked by varying the nickel cross sections in Group 2 [where the (n,p) cross section is important] and in Group 7 where the well-known nickel resonance is prominent. It was found that variations up to the extreme limits of the estimated cross section values resulted in a reactivity change of less than $\frac{1}{2}$ % in k_{eff}. Thus, the final reactivity values will not be severely affected by corrections in cross section values made within these limits in the course of performing and analyzing the results of critical experiments.

Transport theory calculations using a linear anisotropic scattering term for hydrogen show a higher reactivity than do similar diffusion theory calculations. The source of the discrepancy is not known at this time.

2. Critical Experiment

A $\frac{5}{8}$-in. diameter ball-type antimony source has been selected for the AARR critical experiment. This will make it possible to use an existing source drive with suitable modifications.

An initial attempt at electron beam welding of experimental low-cost critical experiment fuel elements was unsuccessful. However, the method still appears promising, and further attempts will be considered using equipment more specifically designed for the AARR critical fuel plates. Tests on a resistance welding technique have also been made, but results have not yet been evaluated. Samples of fuel plates assembled with rubber-base glue have withstood an additional four weeks in room temperature water with no sign of seal failure.

The design of supports for the core and control rod drives for the critical experiment has been completed.

The experimental stepping-motor control rod drive unit (see Progress Report for August, 1962, ANL-6610, p. 63) has been cycled 8,600 times without failure. This test is continuing.

B. Conduction-cooled Reactor as a Substitute for Isotope Heat Sources

The limited supply of relatively long half-life isotopes having a reasonably high power density, and the low conversion efficiencies attainable with thermoelectric devices, has so far limited the power output of isotope-fueled power sources to several tens of watts. In addition, the high cost of

the available isotopes results in a very large expense for isotope-fueled generators producing several hundred watts. It is proposed that a small minimum-weight reactor cooled by conduction would be an attractive alternate to the isotope power supplies in the several hundred watt size range. Accordingly, this study is directed toward the selection of a fuel and moderator for such a reactor system and the preliminary design of the electrical converter and radiator (the latter for a space environment). The nominal size of the power plant is 200 watts electric. With a thermoelectric conversion efficiency of 4%, this requires a reactor thermal output of 5000 watts.

1. Physics

On the basis of the physics work done thus far, a plutonium-fueled, beryllium-moderated, and reflected system appears attractive. A system with a Be:Pu ratio of about 5, and a critical mass of about 18 kg of plutonium has a much higher thermal rating than a solid core of pure plutonium (fast system) since the plutonium-beryllium alloy of this composition has a melting point of about 1600°C. This value is higher than the melting points of either of the pure components. Further, the size of this system (i.e., outer radius of about 10 cm) gives a heat flux at the surface of the thermoelectric elements of about 4 w/cm^2 which is within the design range of current thermoelectric conversion units.

2. Thermoelectric Converter Optimization

The thermoelectric converter utilizes n and p doped lead-telluride elements. The thermoelectric converter is optimized for maximum power output rather than maximum efficiency. The following is a summary of the characteristics of a thermoelectric converter for producing 200 watts of electric power.

Table XI. Lead-Telluride Thermopile Converter Design Parameters

Power Output, watts	200
Output Voltage, volts	12
Hot Junction Temperature, °C	593
Cold Junction Temperature, °C	343
Thermal Efficiency, %	4.0
Number of Couples	207
Length of Couple Arms, cm	1.0
Diameter of n-Couple, cm	1.45
Diameter of p-Couple, cm	1.92
Total Weight of Converter, kg	8.5

3. Radiator Design

The radiator is in close thermal contact with the thermoelement cold junctions. The radiator material is beryllium. Since the heat flux at the outside surface of the spherical heat source and converter is larger than can be discharged by radiation to maintain the desired cold junction temperature, it is necessary to add fins to the surface. The configuration chosen for analysis is a single large fin attached along an equator of the sphere. The equations, which are non-linear, are being programmed for solution on the analog computer. Preliminary analytic solutions of linearized versions of the equations indicate that a satisfactory radiator will weigh about 10 kg.

4. Complete Power Plant

Using the plutonium-beryllium moderated and reflected reactor, the thermoelectric converter described, and a beryllium radiator, the weight breakdown for the power plant is as follows:

Reactor	26 kg
Thermoelectric Converter	8.5 kg
Radiator	10 kg
Total Power Supply	44.5 kg

This excludes the weight of a control system, but it is believed that this will not add more than a few additional kilograms.

VI. NUCLEAR SAFETY

A. Thermal Reactor Safety Studies

1. Metal Oxidation and Ignition Studies

Ignition studies of spherical zirconium powder are continuing. Studies are being made in $\frac{1}{4}$-inch, $\frac{3}{8}$-inch, and $\frac{1}{2}$-inch diameter crucibles of ignition temperature as a function of particle size and sample depth. A completed series of experiments with -140 +170 mesh powder show that the ignition temperature decreases with increasing sample depth. Attempts will be made to account mathematically for the effect of the depth of the powder bed. A similar series of experiments is underway using -325 +400 mesh powder.

Some measurements have been carried out on the effects of dibromotetrafluoromethane[1] (Freon 114B2) on the combustion of uranium and zirconium foil strips. Burning propagation velocities, burning temperatures, and ignition temperatures were measured in air containing two and four percent of this compound. The values obtained are compared with some previously reported results in Table XII. Freon 114B2 is one of the

Table XII. Effects of Various Contaminants on Combustion of U and Zr Foils

Contaminant	Burning Curve Ignition Temperature (For Contaminant Concentration in Air =2%)	Velocity and Maximum Temperature of Burning Propagation Contaminant Concentration in Air			
		2%		4%	
		v, cm/sec	T, C	v, cm/sec	T, C
I. U Foil (0.013 x 0.3 cm)					
None	380	0.52	1375	0.52	1375
CF_2Br-CF_2Br (Freon 114B2)	320	0.36	1110	0.24	1025
CH_3CHF_2	350	Propagation did not occur.			
CF_3Br	285	0.39	1205	0.38	1150
CH_2BrCl	320	0.39	1210	0.31	1150
II. Zr Foil (0.002 x 0.3 cm)					
None	-	2.20	1595	2.20	1595
CF_2Br-CF_2Br (Freon 114B2)	-	Propagation did not occur.			
CH_3CHF_2	-	1.47	1235	1.40	1265
CF_3Br	-	Propagation did not occur.			
CH_2BrCl	-	1.61	1425	Propagation did not occur.	

[1] At the suggestion of Mr. R. B. Smith, AEC (Washington).

most effective compounds tested although it is not as effective as CH_3CHF_2 on uranium. The burning curve ignition temperature was reduced by Freon 114B2 by about the same amount as by many of the other halogenated agents. This substance has the advantage over CH_3CHF_2 of being non-flammable. In the zirconium case, Freon 114B2 prevented propagation as did a number of other compounds tested.

Some interesting differences have been found between the X-ray diffraction patterns of the oxides formed on uranium at 300° and at 600°C. The high temperature oxide yielded a sharp, well developed UO_2 pattern while the lines of the 300°C sample, although like those of UO_2, were broad and asymmetric. A relationship between this finding and the observed change in oxidation kinetics at 450°C (see Progress Report, June 1962, ANL-6580, page 52) is being sought.

2. Metal-Water Reaction Studies

Studies of the reaction of solid uranium with steam by the volumetric method are continuing. In these studies, steam at 1 atm is passed over metal cubes supported on an insulated thermocouple. Steam is condensed and the hydrogen generated by metal-water reaction is measured volumetrically. Results were reported previously for reaction of steam with pure uranium up to 1200°C (see Progress Report, May 1962, ANL-6573, pages 51 and 52). Experiments have now been completed in which steam was reacted with pure uranium at temperatures up to 1500°C and uranium - 1% aluminum alloy at temperatures up to 1400°C. Preliminary results indicate that aluminum has a negligible effect on the reaction. Results for pure uranium at 1400° and 1500°C do not appear to be consistent with results at lower temperatures. The parabolic rate constants are 50 to 100 percent higher than expected from previous results. For example, at 1400°C the parabolic rate constant was 1360 (ml STP/sq cm)^2/min; previous data would have suggested a value of about 700 (ml STP/sq cm)^2/min. There is either a change in the rate law or a spurious rate effect. Confirmatory studies are in progress.

A program has been prepared for use with the IBM-704 computer to complete the analysis of uranium-water reaction data obtained by the condenser discharge method and the in-pile studies in TREAT. The parabolic rate law obtained by the volumetric method, discussed above, was used in the program. Preliminary results indicated that the condenser discharge studies with uranium wires in room temperature water could be described accurately by the computations, provided a somewhat larger activation energy (25 instead of 18.6 kcal/mole) was inserted into the rate law. Experimental results of runs in heated water were 50 to 100 percent higher than computed values.

B. Fast Reactor Safety Studies

1. Experimental Meltdown Program

In-pile experiments are being performed in the TREAT reactor in order to study the characteristics of failure in fast reactor fuel elements, and to study the mechanisms of fuel movement.

a. Pre-Irradiated Meltdown Samples - The burnup analysis has been made on seven of the samples irradiated in the MTR. Three of the elements were the EBR-II specimens, which were tested to failure in the first series of meltdown tests, and burnup was determined from sample residue. The other four elements were Fermi-A specimens, and burnup was determined from measurements on the monitor wires. The analyses indicated that the burnups were about 50% (or less) of the specified level and were consistent with the results found by gamma-ray counting of sample activity.

Because of the relatively low burnup of the three EBR-II specimens tested in TREAT (about 0.3%, 0.3% and 0.1% for maximum recorded temperatures of 840°C, 910°C, and 1120°C, respectively) it has been decided to rerun the series using elements having appreciably higher burnup. The new series will duplicate the three previous tests and will include a fourth one in which the sample will be exposed to a slow transient until a temperature corresponding to sample failure is reached.

2. Theoretical Analysis

a. Transient Heat Transfer Code ARGUS - The ARGUS (RE-248) transient heat transfer code (ANL-6409, Progress Report, August, 1961) is an IBM-704 Fortran program for calculating temperatures in a cylindrical geometry as a function of time, radius, and axial position. It is a more versatile version of the earlier CYCLOPS code (RE-147) which has been used for calculating TREAT sample temperatures. Two major revisions have been made in ARGUS during the last two months in order to eliminate certain instabilities and inaccuracies discovered in previous use. The revisions were:

(1) Replacement of the algorithm for calculating the temperatures at boundary node points of "thick" (number of node points ≥ 3) regions in order to use the method of Back.[1]

(2) Replacement of the algorithm for calculating the temperatures at all node points of "thin" (three node points, provision for an inner iteration scheme with separate time interval less than that of thick regions, so that convergence of thin regions does not force a uniform and too small time interval for all regions) regions.

---

[1] L. H. Back, J. Heat Transfer, ASME, p. 89 (February, 1962).

An extensive series of test problems has been run to test the new code, both against CYCLOPS and analytical calculations. As a result of an evaluation of the checks, the program is now considered to have reached production status. For problems which are identical on ARGUS and CYCLOPS, the former is slower because it requires additional calculations in processing input data. However, for problems in which the time interval for computing is limited by either a high surface conductance, or convergence requirements for a thin region like the zirconium cladding on a Fermi A element, ARGUS running time can be considerably shorter due to the larger time interval. In one test problem, for example, this feature resulted in an increase in time interval from 0.001 sec to 0.004, with a resulting decrease in running time by nearly a factor of four.

Additional features of ARGUS include the following:

(1) Provision for up to twenty-five concentric regions.

(2) Any region may be either "solid" with space- and time-dependent heat generation, or "coolant" either static or flowing.

(3) Solid material properties are approximated as constants over input temperature ranges, with provision for phase changes.

(4) Coolant properties are approximated by second-order polynomials in temperature.

(5) Heat transfer from surfaces by conduction, convection, radiation, and by boiling is provided.

(6) Coolant flow may be specified as a function of time.

b. Calculation of Thermal Stresses in Cylinders - One of the problems encountered in the use of ceramic reactor fuel is the tendency to crack under thermal stress. Uranium dioxide, especially, has a combination of unfavorable physical properties, including low ductility, a high coefficient of thermal expansion of about $10^{-5}/°C$, a low ultimate strength of about 10,000-20,000 psi, and poor thermal conductivity of about 0.02 watts/cm°C at elevated temperatures. In order to study results of small-scale TREAT testing in a thermal reactor to relate those results to possibly different stress conditions arising in testing of actual fast reactor cores, and to point out potential problem areas for such larger-scale testing, calculations of thermal stresses resulting from transient temperature distributions are necessary.

A Fortran code 1560/RE was written for the IBM-704 to calculate thermal stresses in a right circular cylinder with constant values of elastic modulus and thermal expansion, for an arbitrary radial temperature

distribution. Print-out includes radial, polar and axial stresses and radial displacements at the given radial node points, as well as the stored mechanical energy per unit length (calculated on the basis that the stored energy per unit volume is one-half the product of stress and strain). The equations used are valid except near the ends of the cylinder, i.e., within about one diameter from each end. This condition is not met properly for typical pressed and sintered pellets with length-to-diameter ratios ≤ 2. However it is satisfactory for longer extruded oxide cylinders, and can give qualitative indication of conditions near the radial mid-plane of short pellets.

VII. PUBLICATIONS

Papers

PHOTOGRAPHIC DETECTORS FOR NEUTRON DIFFRACTION
Harold Berger
Rev. Sci. Instr. 33 844-846 (Aug. 1962)

FOR NONDESTRUCTIVE TESTING ... NEUTRON RADIOGRAPHY
Harold Berger
Nucleonics 20 (9) 77-81 (Sept. 1962)

ALUMINUM ALLOYS WITH IMPROVED HIGH TEMPERATURE AQUEOUS CORROSION RESISTANCE
J. E. Draley, W. E. Ruther, and S. Greenberg
J. Nuclear Materials 6 (2) 157-171 (July 1962)

FLUORINE BOMB CALORIMETRY: IV. THE HEATS OF FORMATION OF TITANIUM AND HAFNIUM TETRAFLUORIDES
E. Greenberg, J. L. Settle, W. N. Hubbard
J. Phys. Chem. 66 1345-1348 (July 1962)

MAGNETIC SUSCEPTIBILITY OF ReF_6
H. Selig, F. A. Cafasso, D. M. Gruen, and J. G. Malm
J. Chem. Phys. 36 3440-3444 (June 15, 1962)

ROLE OF CERIUM IN THE SUPPRESSION OF GAMMA-RAY-INDUCED COLORING OF BORATE GLASSES
A. M. Bishay
Journal of the American Ceramic Society 45 389-393 (1962).

GAMMA-RAY-INDUCED COLORING OF GLASSES IN RELATION TO THEIR STRUCTURE
A. M. Bishay and K. R. Ferguson
Advances in Glass Technology, pp 133-148, Technical papers of the Sixth International Congress on Glass, July 8-14, 1962, Washington, D. C. Compiled by the American Ceramic Society, Columbus, Ohio, Plenum Press, New York (1962).

IN-PILE PHOTOGRAPHIC STUDIES OF EBR-II MARK-I AND FERMI CORE - A SAMPLE MELTDOWN
C. E. Dickerman, G. H. Golden, and L. E. Robinson
Nuclear Sci and Eng. 14 30-36 (1962)

The following papers were presented at the Seminar on Physics of Fast and Intermediate Reactors, Vienna, August 3-11, 1961, and have now been published in Proceedings, 1962 International Atomic Energy Agency, Vienna:

REACTIVITY COEFFICIENTS OF SODIUM IN SOME LARGE FAST REACTORS
M. G. Bhide and H. H. Hummel
Vol. II, pp. 177-186

PERFORMANCE OF LARGE FAST POWER REACTORS, INCLUDING EFFECTS OF HIGHER ISOTOPES, RECYCLING AND FISSION PRODUCTS
D. Okrent
Vol. II, pp. 271-297

THE PHYSICS ASPECTS OF A COUPLED FAST-THERMAL STEAM SUPERHEATING REACTOR
B. J. Toppel and R. Avery
Vol. II, pp. 373-407

STABILITY ANALYSIS OF EBR-II
H. H. Hummel and L. T. Bryant
Vol. III, pp. 107-117

A REVIEW OF THE NUCLEAR ASPECTS OF FAST-REACTOR SAFETY
D. Okrent
Vol. III, pp. 155-169

THE FAST-REACTOR SAFETY PROGRAMME IN TREAT
C. E. Dickerman, D. Okrent, and E. Sowa
Vol. III, pp. 171-193

MAJOR ACCIDENT ANALYSES FOR EXPERIMENTAL ZERO-POWER FAST REACTOR ASSEMBLIES
G. Fischer, E. W. Barts, S. Kapil, and K. Tomabechi
Vol. III, pp. 195-207

A THEORETICAL STUDY OF DESTRUCTIVE NUCLEAR BURSTS IN FAST POWER REACTORS
V. Z. Jankus
Vol. III, pp. 209-238

THE PHYSICS DESIGN OF EBR-II
W. B. Loewenstein
Vol. III, pp. 263-314

ANL Reports

ANL-6274 FABRICATION OF EBR-II, CORE-I FUEL PINS
H. F. Jelinek

ANL-6414 PROGRESS REPORT ON NONDESTRUCTIVE TESTING BY ELECTROMAGNETIC METHODS
C. J. Renken

ANL-6428 THE EFFECTS OF IRRADIATION ON SOME BINARY ALLOYS OF THORIUM-PLUTONIUM AND ZIRCONIUM-PLUTONIUM
J. A. Horak, J. H. Kittel, and H. V. Rhude

ANL-6429 THE EFFECTS OF IRRADIATION ON URANIUM-PLUTONIUM-FISSION FUEL ALLOYS
J. A. Horak, J. H. Kittel, and R. J. Dunworth

ANL-6431 IRRADIATION BEHAVIOR OF RESTRAINED AND VENTED URANIUM-2 w/o ZIRCONIUM ALLOY
J. A. Horak, J. H. Kittel, and F. L. Yaggee

ANL-6475 KINETICS OF THE REDUCTION OF URANIUM OXIDES BY CARBON MONOXIDE AND BY HYDROGEN
Milton Volpe and Slavko Mihailovich

ANL-6529 THORIA AND THORIA-URANIA REINFORCED BY METAL FIBERS
Y. Baskin and J. H. Handwerk

ANL-6555 2D PERT: A TWO-DIMENSIONAL PERTURBATION CODE
J. M. Chaumont and J. A. Koerner

ANL-6582 TWO SPHERICAL FAST CRITICAL EXPERIMENTS (ZPR-III Assemblies 38 and 39)
J. C. Bates, W. G. Davey, P. I. Amundson, J. M. Gasidlo, J. K. Long, and W. P. Keeney

ANL-6585 POSSIBLE IMPLICATIONS OF THE DAMAGE BY RADIATION IN THE STORAGE OF PROPELLANTS IN OUTER SPACE AND TENTATIVE METHODS FOR ITS MEASUREMENT
J. A. McMillan

ANL-6587 PHYSICS ANALYSIS OF THE JUGGERNAUT REACTOR
D. P. Moon

ANL-6595 A SUBCRITICAL PLUTONIUM-FUELED FAST REACTOR CORE (ZPR-III Assembly 37)
P. I. Amundson, R. Jiacoletti, J. K. Long, and R. L. McVean

ANL-6604 STABILIZED RELAXATION OSCILLATOR
Charles Erwin Cohn